Journal of Hydrology X 21 (2023) 100155

Contents lists available at ScienceDirect

Journal of Hydrology X

journal homepage: www.sciencedirect.com/journal/journal-of-hydrology-x

Research papers

Extension of the Gardner exponential equation to represent the hydraulic conductivity curve: Inclusion of macropore flow effects

Theophilo Benedicto Ottoni Filho [a], Anderson Rodrigues Caetano [a], Marta Vasconcelos Ottoni [b,*]

[a] Department of Water Resources and Environment, Universidade Federal do Rio de Janeiro (UFRJ), Rio de Janeiro, RJ, Brazil
[b] Geological Survey of Brazil, Companhia de Pesquisa de Recursos Minerais (CPRM), Rio de Janeiro, RJ, Brazil

ARTICLE INFO

Keywords:
Hydraulic conductivity modeling
Preferential flow
Matrix flow
Gardner exponential model

ABSTRACT

In soil hydraulics, it is crucial to establish an accurate representation of the relative hydraulic conductive curve (rHCC), K_r(h). This paper proposes a simple way to determine K_r(h), called the Modified Gardner Dual model (MGD), using a logarithmic extension of the classical Gardner exponential representation and including macropore flow effects. MGD has five parameters which are hydraulic constants clearly identified in the bilogarithmic representation of K_r(h). Two of them are related to the main inflection point coordinates of rHCC; from them, it is possible to determine the macroscopic capillary length of the infiltration theory. The model was tested in the suction interval $0 < h < 15{,}000$ cm with a total of 249 soil samples from two databases, and employing a flexible representation of the Mualem-van Genuchten (MVG) equation as a reference. Using the RMSE statistics (with log base) to measure the fitting errors, we obtained a 31% reduction in errors (RMSE_MGD = 0.27, RMSE_MVG = 0.39). In 74% of the soils, including samples from the two databases, the reduction was 53% (RMSE_MGD = 0.19, RMSE_MVG = 0.40); the rHCC data fitting of this group was accurate over all the suction h intervals, with RMSE_MGD < 0.32 in each soil sample. In the remaining 26% of the samples, the quality of the MGD fitting degraded due mainly to the presence of multiple rHCC data inflection points. Therefore, in soils without this structural peculiarity, the proposed model revealed to be quite accurate in addition to being analytically simple. Another advantage of MGD is that its parameters depend mainly on the data with h around and lower than the main inflection suction value, which, in turn, never exceeded the 300-cm limit in this study. Hence, in soils that do not have multiple inflections, the extrapolations of the model in drier intervals (1000 cm < h < 15,000 cm) are reliable. The MGD parameter optimization software has been called KUNSAT. It is available in the Supplementary Material or from the corresponding author on request.

1. Introduction

Since, by Darcy's Law, water flow is the product of hydraulic conductivity K and the hydraulic gradient, the determination of the K(h) curve of variation of K with suction h is a priority in soil hydrology and in flow and transfer modeling in non-saturated soils. As, according to Darcy's Law, K errors have a potential to introduce errors with the same magnitude in water flow, developing accurate models to represent K(h) is of capital importance. Emphasizing the relevance of the accurate determination of K(h), it is important to take into account that in hydrologic processes, with the change in the water content (θ) in the pores, K(h) normally presents a variation of various orders of magnitude. In this paper, we considered saturated hydraulic conductivity (K_s) to be a known parameter so that it will suffice to know the relative hydraulic conductivity curve (rHCC), $K_r(h) = K(h) / K_s$. Suction h ($h \geq 0$, h in cm) is the symmetric value of the matrix potential.

Numerous representations of rHCC have been proposed since the 1950 s based on purely empirical models, or semi-empirical conceptual physical/hydraulic models obtained mainly from either the soil particle size distribution curve or the water retention curve (WRC), θ(h) (Assouline & Or, 2013; Gardner, 1958; Leij et al.,1997; Raats & Gardner, 1971; Rudiyanto et al., 2020; Weynants et al., 2009). The most promising models are those involving the direct fitting of their parameters to experimental data (h,K_r), either associated or not with the fitting of the WRC representation parameters. Among the rHCC models involving suction intervals from saturation to the wilting point [$\theta(h = 15000$ cm)], the Mualem-van Genuchten model (MVG) (Vereecken et al., 2010) is probably the most used. In its more flexible and accurate form

* Corresponding author.
E-mail address: marta.ottoni@sgb.gov.br (M.V. Ottoni).

https://doi.org/10.1016/j.hydroa.2023.100155

Available online 17 August 2023
2589-9155/Published by Elsevier B.V. This is an open access article under the CC BY-NC-ND license (http://creativecommons.org/licenses/by-nc-nd/4.0/).

(Vereecken et al., 2010), it has the following representation:

$$K_r = K_{ro} S^L \left[1 - \left(1 - S^{(n/(n-1))}\right)^{(1-1/n)}\right]^2 \quad (1a)$$

$$S = S(h) = [1 + (\alpha h)^n]^{-(1-1/n)} \quad (1b)$$

$$S = [\theta(h) - \theta_r]/(\theta_s - \theta_r) \quad (1c)$$

where S is the effective saturation, K_{ro} ($0 < K_{ro} \leq 1$) and L (negative, null or positive) are dimensionless soil data [(h,K_r)] fitting parameters, and θ_s, θ_r, n (all three dimensionless, $n > 1$) and α (cm^{-1}) are positive soil parameters (with the exception of the residual moisture, θ_r, which can be null) of the θ(h) curve adjustment. Another popular analytically simple equation of representation of K_r(h) with large application in infiltration flows is the Gardner exponential model (Gardner,1958):

$$K_r = e^{(-h/\lambda)} \quad (2)$$

where e is the Napier constant and λ (cm), the macroscopic capillary length (White & Sully, 1987), a physical parameter related to the soil sorptivity and K_s, according to infiltration theory (Ottoni Filho et al., 2019; Vandervaere, 2002; White & Sully, 1987). Eq. (2) is popular mainly because it makes the linearization of the Richards differential equation (Richards, 1931) possible, both for steady and unsteady flows (with greater restriction in the latter) (Assouline & Or, 2013; Philip, 1969; Russo, 1988; Warrick, 1974). This makes the analytical solution of problems involving infiltration flows possible, such as happens with the popular ring and disk infiltrometers, as well as with permeameters (Ankeny et al., 1991; Reynolds, 2008a; Reynolds, 2008b; Reynolds, 2008c; Smettem & Clothier, 1989; Wooding, 1968). This allows the determination of hydrodynamic parameters K_s and λ in the field using the small h values imposed by those devices. However, despite the simplicity of Eq. (2), it has the disadvantage that its application is limited to suction intervals close to saturation (Communar & Friedman, 2014; Gardner, 1958; Jarvis & Messing, 1995; Leij et al., 1997). Ottoni Filho et al. (2019) corroborated this fact when they observed that Eq. (2) could be applied properly to 77 soils close to saturation, but only in suction intervals not exceeding the 300-cm limit. However, these wet intervals influence the infiltration flows the most, which lends consistency to the large applicability of Eq. (2) in infiltrometry and permeametry.

It is even improbable that a simple empirical law such as Eq. (2) succeeds in representing the depletion of K_r from saturation in large suction variation intervals, resulting from the reduction in size (thickness of water in voids) and the variation of the geometric and hydraulic complexity of the hydrated system of voids. The assumed capillary configuration of the hydrated pore space close to saturation must continue to vary its diameter scale and geometric and hydraulic complexity with the decrease in moisture and increase in suction; the capillary configuration must become less predominant in terms of influence on the hydraulic conductivity than other configurations foreseen, such as the corner and film flow (Assouline & Or, 2013; Lebeau and Konrad, 2010; Peters & Durner, 2008; Tuller & Or, 2001). Seeking to obtain a simple analytical representation of the depletion of rHCC in greater suction intervals, Ottoni Filho et al. (2019) proposed that for h values higher than a given suction h_o, called transition suction, the scale of the variables of the exponential depletion of Eq. (2) changed from linear to logarithmic, both for K_r and h. This is the fundament of the Gardner Dual (GD) model proposed by Ottoni Filho et al. (2019), corresponding to the following extrapolation of the Gardner exponential equation ($\log = \log_{10}$):

$$K_r(h) = e^{(-h/\lambda)}, h \leq h_o \quad (3a)$$

$$\log K_r(h) = a + b e^{[-(\log h)/\beta]}, h \geq h_o \quad (3b)$$

where β is a positive constant (dimensionless), called the conductive depletion coefficient, and a and b are constants to be determined so that K_r(h) is continuous and smooth at h_o. Making $Y = \log K_r$; $X = \log h$, $Y_o = Y(h_o)$; $X_o = X(h_o)$; $g = h/h_o$, the following resulting dual function, $d_\beta(g) = Y/Y_o$, can be considered to be an expression of a normalized rHCC (Ottoni Filho et al., 2019), dependent only on β, and that incorporates Eq. (2):

$$d_\beta(g) = g, 0 \leq g \leq 1, \quad (4a)$$

$$d_\beta(g) = 1 + (\beta/\log e)[1 - g^{-(\log e)/\beta}], g \geq 1 \quad (4b)$$

Ottoni Filho et al. (2019) tested GD with 153 soils from the UNSODA database (Leij et al., 1996). The quality of fitting to the experimental data was high in half of the soils (77), similar to that presented in the curve in Fig. 1, with a mean RMSE [defined in Eq. (18)] of 0.19 in this group of soils, a promising result [the same mean error for the MVG model of Eq. (1) was 0.52]. It was disappointing that the fitting errors of the other half of the samples (76 soils) was three times as large (mean RMSE of 0.57). As a justification of this fact, the authors realized that in the group of 76 samples the rHCC experimental data close to saturation tended not to converge to the origin ($X = 0$, $Y = 0$) of the XY coordinate axis (that is, to saturation) asymptotically to the axis of $X = \log h$, in contrast to the soil in Fig. 1 and, apparently, also to the other soils well fitted by GD. In the 76 soils with poorer fitting, one can notice a frequent tendency to a sharp reduction of the K_r data close to saturation, many times greater than two orders of magnitude, in a very narrow suction interval (Fig. 7 in Ottoni Filho et al., 2019), in the 0–10-cm range, which is a typical characteristic of soils with macropore flow (MF) (or fast flow). According to Ottoni Filho et al. (2019), the MF phenomenon was the main cause of deterioration of the quality of fitting of GD.

However, soils with MF are common. Due to their relevant and frequent hydrologic and hydraulic features in terms of water flows and mass transport and pollution after wetting events, these soils are extensively studied and modeled in relation to their pore structure, hydraulics, pedology and physical chemistry (Beven & Germann,1982, 2013; Gerke et al., 2013,2010; Gerke & van Genuchten, 1993; Jarvis, 2007; Jarvis et al., 2016; Zhang et al., 2018). Their pore structure typically presents a dual permeability field close to saturation: one where the MF results from a macropore network (biopores, interaggregate voids, shrinkage or mechanical cracks) with small volume within the bulk soil volume, but that produces a predominant hydraulic conductivity in general, in relation to the second field. The second field of permeability is the one that generates the matrix flow, which predominates volumetrically in the bulk soil volume, but that produces a usually small saturated hydraulic conductivity in relation to the soil K_s (it can be a few orders of magnitude smaller than K_s). Therefore, it is improbable that a robust model of representation of rHCC exists for study purposes involving soil wetting and draining that does not take the MF effects into account.

The MF hydraulics has been mathematically modeled by various methods (Beven & Germann, 2013; Jarvis, 2008; Jarvis et al., 2016; Lassabatere et al., 2014; Sternagel et al., 2019). A practical possibility is the modification of a current model of representation of rHCC aiming at incorporating the MF effects close to saturation, such as in Schaap & van Genuchten (2006) with the MVG model. The objective of this study was to modify the GD model by Ottoni Filho et al. (2019) to incorporate the MF effects and make it more general and accurate. The new model, called the Modified Gardner Dual model (MGD), will be evaluated with two independent databases (one international and another regional) with 249 samples using the MVG model of Eq. (1) as a reference. MGD will be applied to suction intervals from saturation to the wilting point [θ(h = 15,000 cm)].

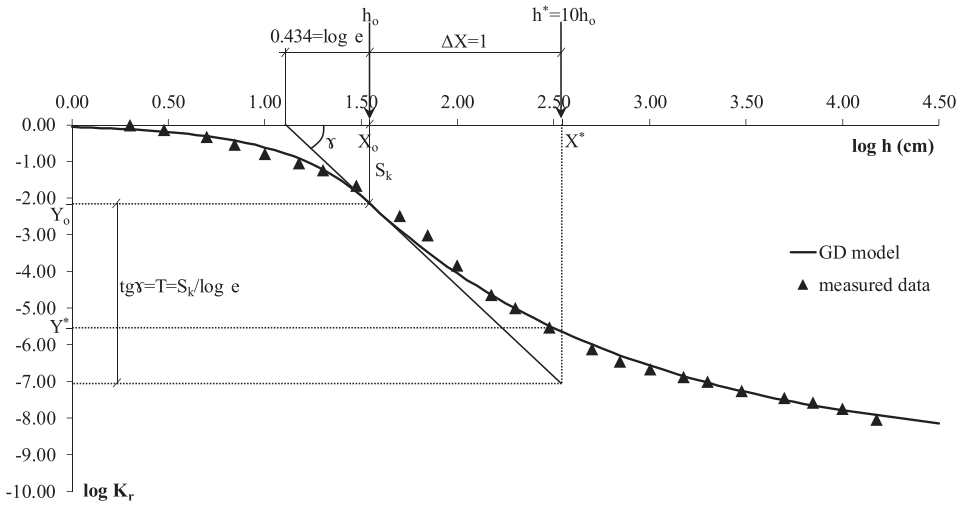

Figure 1. Typical example [soil 4661 from the UNSODA database (Leij et al., 1996)] of the bilogarithm representation of the experimental data of the $K_r(h)$ curve obtained with the GD model. One can notice a clear tendency of inflexion of the data around suction ho = 35 cm. The figure shows the S_k index = $-Y_o = 2.14$. From Eq. (6), $\lambda = 7.09$ cm. Parameter $\beta = 1.38$ is better identified in Fig. 2 (Source: Ottoni Filho et al., 2019).

2. Material and methods

2.1. Gardner Dual Model: review and comments

The GD model (Ottoni Filho et al., 2019) focuses on the determination of the point (X_o,Y_o) of rHCC represented in the bilogarithmic scale (Fig. 1). It can be noted that the plot of the experimental pairs of this curve usually has an inflection in the wet interval of suctions and GD confirms that it is the h_o parameter that defines the position of this inflection (Fig. 1). The value of $S_k = -Y_o = -\log K_r(h_o)$, $S_k > 0$, called the conductive depletion index, is the second parameter of the model. Coincidentally, S_k is proportional to the absolute value of the dY/dX derivative at h_o (Fig. 1). S_k was defined in relation to the rHCC curve in a way similar to that of the Dexter S index established for WRC (Dexter, 2004) (the latter is acknowledged to be a soil structural index), since (ln is the natural logarithm):

$$S_k = -dY/d(\ln h)(h = h_o) \quad (5)$$

Another peculiarity of GD pointing out the hydraulic importance of the inflexion point (X_o,Y_o) of rHCC is that λ, the macroscopic capillary length, can be calculated from (X_o,Y_o), since:

$$\lambda = (\log e)h_o/S_k \quad (6)$$

which associates rHCC to the infiltrometry and permeametry, which determine λ and K_s. The GD model also indicates that when $h > h_o$, the porous medium becomes hydraulically more complex to describe in terms of viscous forces, as a third parameter, β, becomes necessary to quantify the hydraulic conductivity. However, in the same way that the simple exponential model of Eq. (2) cannot represent $K_r(h)$ accurately at suctions higher than h_o (Ottoni Filho et al., 2019), we do not believe that the simplicity of the GD model may be effective in very dry moisture ranges, at very high suction values. For example, above h = 15,000 cm (suction at wilting point), where, in general, the most common models of calculation of rHCC are no longer accurate (Lebeau & Konrad, 2010; Peters, 2013; Peters et al., 2023; Rudiyanto et al., 2020; Tuller & Or, 2001; Zhang, 2011).

The influence of parameter β on the representation of rHCC can be better visualized in the graph (Fig. 2) of the family of normalized functions, $d_\beta(g)$ (d_β in the decimal scale and g in the logarithmic scale). As $d_\beta = \log K_r/\log K_r(h = h_o)$ and $g = h/h_o$, the shapes of both curves (d_β vs. log g and log K_r vs. log h) are equal and inverted. Fig. 2 thus shows the influence of β on the shape of rHCC. This influence is better characterized by parameter f(β) [function f expressed by Eq. (27) in Ottoni Filho et al., 2019], called the linearization fraction [$0 < f(\beta) < 1$]. The linearization fraction, as its name suggests, must be seen as an easily identifiable parameter of rHCC: the closer it is to one, the more

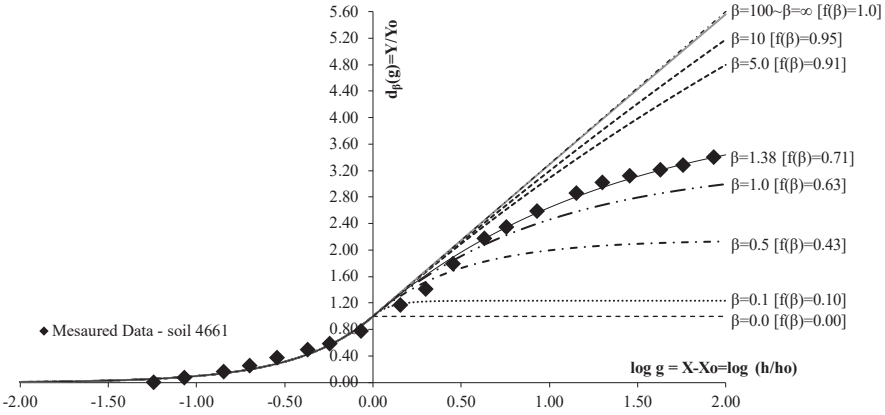

Figure 2. Family of normalized curves, $Y/Y_o = d_\beta(g)$, of the relative hydraulic conductivity, representing the totality of the shapes of $Y = K_r(h)$ for the GD model. The soil in Fig. 1 is identified in the figure as an illustration.

rectilinear (less curved) is the $h > h_o$ branch of the curve close to its inflexion (X_o,Y_o); the closer it is to zero, the more curvilinear it is. Therefore, we conclude that the convex form [Y(X) branch close to saturation, $h < h_o$], coupled with the following linear branch ($h > h_o$) presented by the Y(X) curve of the MVG model (Ottoni Filho et al., 2019) is a particular case [f(β) around 1] of a more general shape represented by the GD model. For the sake of illustration, Fig. 2 presents the experimental data of the soil in Fig. 1 and its corresponding $d_\beta(g)$ curve ($\beta = 1.38$).

2.2. Modified Gardner Dual Model: model development and description

The new model, MGD, includes the effects of MF in GD by adding two parameters (M and h_a), described below, to the three parameters of GD (h_o, S_k and β). It is proposed that MGD uses the results of GD when the latter is adequate to represent rHCC. Ottoni Filho et al. (2019) observed that when the RMSE fitting error of GD [Eq. (18)] to the rHCC experimental data of a given soil was lower than 0.32, the $K_r(h)$ function generated by the model, like the curve in Fig. 1, produced small errors of representation of the rHCC data, without bias, over the whole interval of h tested. Therefore, when the RMSE calculated from GD is smaller than 0.32, MGD calculates $K_r(h)$ in the same way GD does, and the two new parameters (M and h_a) are null, that is, the MF effects in the soil are considered not relevant.

2.2.1. Characterization of parameter M

We know that the MF effects are relevant only in a very narrow interval of suctions close to saturation. Based on a detailed bibliographic study, Jarvis (2007) reported that pore spaces corresponding to capillaries with equivalent diameters smaller than 0.3 mm, and that generate suctions >10 cm (from the Laplace equation), are generally sufficiently small not to hold relevant MF. Therefore, here we will suppose that when $h \geq 10$ cm, all the flux is due to the matrix flow (mF). However, when MF exists, the saturated hydraulic conductivity due to mF, K_{sm}, is smaller than K_s, as already remarked in the Introduction. The new parameter M ($M \geq 0$), called macropore flow exponent, is defined here as a dimensionless value related to K_s and K_{sm} by the expression below:

$$10^M = K_s/K_{sm} \tag{7}$$

We propose that the mF-relative hydraulic conductivity curve (identified as rmHCC):

$$K_{rm}(h) = K_m(h)/K_{sm} \tag{8}$$

where K_m is the hydraulic conductivity due to mF, be modeled by the same dual equation [Eq. (3)] of calculation of the hydraulic conductivity depletion in model GD, substituting $K_r(h)$ in Eq. (3) with $K_{rm}(h)$. From a new notation (in relation to the GD model): $Y = \log K_{rm}$; $Y_o = Y(h = h_o)$, we conclude, as a consequence of the GD model, that

$$Y(g)/Y_o = d_\beta(g), g = h/h_o \tag{9}$$

where $d_\beta(g)$ is the dual function of Eq. (4), here called the depletion function. With the Y and Y_o new notation used above, the three parameters (h_o, S_k, β) of the GD model and their names are kept in MGD as matrix flow parameters, just like the relation below, already mentioned in Section 2.1:

$$S_k = -Y_o \tag{10}$$

and Eqs. (5) and (6) remain valid. Obviously, when $M = 0$, GD is a particular case of MGD, because, from Eq. (7), $K_{sm} = K_s$.

What is actually sought to model with MGD is rHCC, which we have now given the new notation:

$$Y^*(h) = \log K_r(h) = \log[K(h)/K_s] \tag{11}$$

taking into account that $Y_o^* = Y^*(h = h_o)$. As we considered that if $h \geq 10$ cm, $K = K_m$, then according to Eqs. (7), (8) and (11):

$$Y^* = Y - M, \; for\, h \geq 10cm \tag{12}$$

Thus, when $h \geq 10$ cm, curves $K_r(h)$ and $K_{rm}(h)$ will be coincident in a bilogarithmic graphic representation if the scale of Y* is shifted downwards M units on the vertical axis (Fig. 3). Based on the results from Ottoni Filho et al. (2019), we will assume $h_o \geq 10$ cm. With the exception of β, the other parameters of MGD can be graphically represented (Fig. 3), showing the close relationship between these parameters and the optimized rHCC. The inflection points of both curves, rHCC and rmHCC, occur at the transition suction, h_o. From Eqs. (10) and (12):

$$-Y_o^* = M + S_k \tag{13}$$

2.2.2. Characterization of parameter h_a

The MF effects are generally restricted to very narrow suction intervals close to saturation, as already mentioned. According to a review by Jarvis (2007), the maximum suction values (h_{max}) capable of generating relevant MF are in the order of 6 to 10 cm, depending on the soil. To develop a simple method of calculation of $K_r(h)$ in the h interval where MF occurs, we set a single value of $h_{max} = 10$ cm for the MGD model. In later work, Jarvis (2008) developed a power function [his Eq. (11)] to represent $K_r(h)$ in the MF suction interval using a minimum suction (h_{min}) value that allows entry of air into the largest pores; in this case, when $h \leq h_{min}$, $K = K_s$. Jarvis (2008) utilized laboratory and field experiments and evaluated that his model calculated the $K_r(h)$ function in the [h_{min}, h_{max}] interval properly. In the MGD model, the h_{min} constant will be an MF parameter of the soil, called air-entry suction, h_a ($0 < h_a < 10$ cm). Therefore, applying logarithm to Jarvis's Eq. (11), Y*(log h) is expected to vary linearly in the suction interval [h_a,10 cm], decreasing between $Y^* = 0$ and $Y_{10}^* = Y^*(h = 10$ cm), as represented schematically in Fig. 3. From Eqs. (6), (9), (10) and (12):

$$-Y_{10}^* = 10\,S_k/h_o + M = 10\log(e)/\lambda + M \tag{14}$$

Therefore, if $M > 0$, the representation of $Y^* = \log K_r(h)$ in MGD is:

$$Y^* = 0, 0 \leq h \leq h_a \tag{15a}$$

$$Y^* = Y_{10}^*[1 - (1 - \log h)/(1 - \log h_a)], \; h_a \leq h \leq 10\,cm \tag{15b}$$

where Y_{10}^* is as in Eq. (14); and, from Eqs. (9), (10) and (12):

$$Y^* = -S_k d_\beta(g) - M, \; g = h/h_o, \; h \geq 10cm \tag{15c}$$

If $M = 0$, h_a will be considered null and MGD calculates Y* [from Eqs. (9) and (10)] in the same way as GD does:

$$Y^* = Y = -S_k d_\beta(g), \; g = h/h_o, \; h \geq 0 \tag{16}$$

In Eqs. (15) and (16) $d_\beta(g)$ is the depletion function given by Eq. (4) and represented in Fig. 2.

2.3. Soil databases

Two soil databases were used to evaluate the MGD model. The first one was extracted from the UNSODA database (Leij et al., 1996; Nemes et al., 2001), an international database of temperate climate soils from the Northern hemisphere. From UNSODA, Schaap & Leij (2000) selected 235 samples with experimental data of both the θ(h) and $K_r(h)$ curves, in addition to data on K_s, the three USDA textural fractions, and soil density. Data on the same variables were collected from the second database, here called the Vereecken database (Vereecken, 1988), with 136 samples representative of the main types of soils from Northern Belgium (Weynants et al., 2009). Further information on the two databases and methods of determination of the variables can be found in the reference literature. Access to the data above was kindly granted by Dr. Marcel Schaap (UNSODA database) and Dr. Melanie Weynants (Vereecken database); however, satisfactory information on textural fractions and

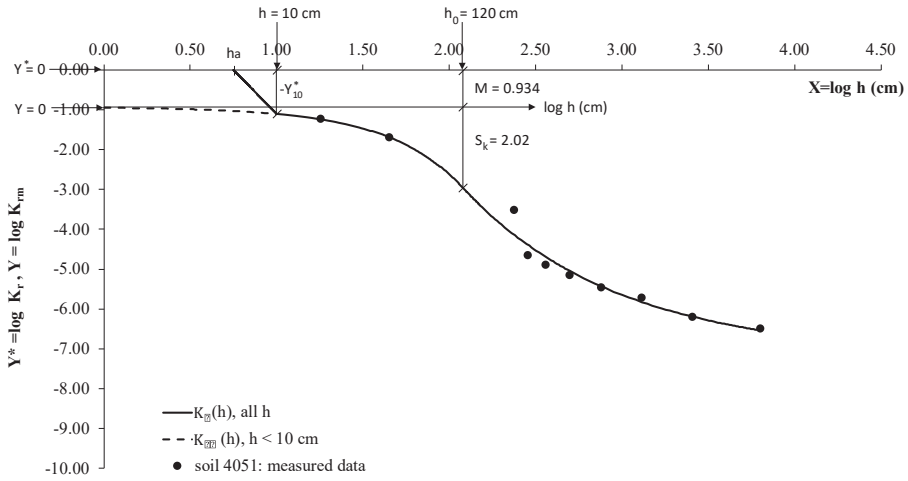

Figure 3. Example (soil 4051 from UNSODA) of the representation of the relative hydraulic conductivity curve, $K_r(h)$ (solid line), by MGD model. The dashed line indicates the relative hydraulic conductivity curve (rHCC) due to matrix flow, $K_{rm}(h)$, in the suction interval [1 cm, 10 cm]. Parameters $h_o = 120$ cm, $S_k = 2.02$ and $M = 0.934$ are represented. Parameter f (β) = 0.604 (from $\beta = 0.900$) is related to the curvature of rHCC at its inflection, according to the representation in Fig. 2. Parameter h_a is the MGD air-entry suction, represented schematically in the figure. Y_{10}^* is an MGD auxiliary parameter, obtained with Eq. (14).

soil density could not be obtained from the second database.

Regarding the UNSODA database, Ottoni Filho et al. (2019) excluded 82 samples from the initial group of 235 samples, reducing it to 153 samples. The authors explained the reasons for this exclusion, but most of the excluded samples (60) were from soils without K_s measurements; instead, these K_s values were determined with pedotransfer functions, which might result in great experimental noise in the rHCC data. Additionally, 12 and 28 samples were excluded from the UNSODA and Vereecken databases, respectively, because they had less than two pairs (h,K_r) measured between the suctions of 10 cm and 45 cm, which will be justified in the next section. Therefore, in this study, the numbers of UNSODA and Vereecken database samples used were 141 and 108, respectively. The measured suction of any sample varied from a minimum of 1 cm to 40 cm to a maximum of around 15,000 cm.

2.4. Parameter optimization and fitting error statistics

According to the first paragraph of Section 2.2, the three matrix flow (mF) parameters (h_o, S_k, β) of MGD will be determined with the algorithm used in GD (Ottoni Filho et al., 2019) when the GD fitting RMSE error [Eq. (18)], considering all the experimental pairs (h,K_r) of the sample, is smaller than 0.32. In this case, the macropore flow (MF) parameters, M and h_a, are considered null and rHCC and the fitting error statistics are calculated as in GD. Therefore, in the next two paragraphs we will consider $M > 0$ and $h_a > 0$, that is, MF exists and Eq. (15) applies.

As to the optimization of M, h_o, S_k and β, the strictly increasing sequence of N1 suctions observed (measured) in the sample, $\{h_i, h_i \geq 10$ cm$\}$, and the corresponding $\{Y_{oi}^*\}$ sequence of observed values of $Y^* = \log(K_r)$, represented by the function described in Eq. (15c), were used. The optimization program maintained the same few restrictions imposed by Ottoni Filho et al. (2019) to the observed suction data of the sample, but required new restrictions: a) eliminate samples with $\{h_i\}$ sequence with less than four elements ($N1 < 4$) or less than two elements $h_i \leq 45$ cm, for data insufficiency; b) eliminate h_i data > 20,000 cm with no interest for the objectives of the study; c) eliminate samples with $\{Y_{oi}^*\}$ sequence with at least one null value, because it is an indication that the soil air-entry suction (h_a) is ≥10 cm, which contradicts an MGD hypothesis. As to the optimization of h_a, the strictly increasing sequences of the observed N2 suctions were used, $\{h_i, h_i < 10$ cm$\}$, as well as the corresponding $\{Y_{oi}^*\}$ sequence, with Y^* calculated with Eqs. (15a) and (15b). In Eq. (15b), Y_{10}^* was considered to be a constant known from Eq. (14) and from the already determined values of M, S_k and h_o. When $N2 = 0$, it will not be possible to optimize h_a due to lack of data.

The conditions above were taken into consideration in the parameter optimization in order to minimize the sum of squared errors (SSE):

$$SSE = \sum_{i=1}^{i=N1,N2..N} [Y^*(h_i) - Y_{oi}^*]^2 \quad (17)$$

where $\{h_i\}$ and $\{Y_{oi}^*\}$, with N1 values, were used in the optimization of (M, h_o, Sk, β), and the corresponding sequences with N2 values, in the optimization of h_a. The software KUNSAT was developed in visual basic with Microsoft Excel® spreadsheets to calculate the optimization algorithm. The algorithm also allowed flexibility in the optimization of the M parameter, making M zero when it is optimized with a negative value; when this happens, parameter h_a is made null and the program optimizes the other three parameters of MGD and calculates the fitting error statistics exactly as in GD.

The KUNSAT software also calculates the fitting error statistics, described below, and plots the fitted rHCC of the sample with a representation of the experimental pairs (h, K_r). This software only requires that the user identify the sample and insert the values of K_s and of the experimental pairs (h, K). KUNSAT is available in the Supplementary Material or from the corresponding author on request.

The dimensionless RMSE (root mean square error) and ME (mean error) statistics below were used to evaluate the fitting errors in samples with N ($N = N1 + N2$) pairs of observed values, (h_i, Y_{oi}^*):

$$RMSE = \sqrt{\frac{SSE}{N-p}} \quad (18)$$

$$ME = \sum_{i=1}^{i=N} \frac{[Y^*(h_i) - Y_{oi}^*]}{(N-p)} \quad (19)$$

where, from the optimized MGD parameters, SSE is calculated from Eq. (17) and Y^* from Eqs. (15) or (16). The p value is the number of degrees of freedom of the mathematical model of representation of rHCC. In the case of MGD (or GD), p is equal to the number of parameters of the model minus one [the need to subtract one arises from the dual nature of Eq. (3), which makes the optimization of λ independent of that of β and vice-versa]. In the case of MVG [Eq. (1)] the statistics of Eqs. (18), (19) and (20) can also be used, where $p = 2$. In MGD, when $M > 0$, $p = 4$ (5–1); when $M = 0$, $p = 2$ (3 – 1). When h_a cannot be optimized ($N2 = 0$), $p = 3$ (4 – 1). The RMSE value indicates the mean absolute error in the sample, while ME indicates a bias to overestimate ($ME > 0$) or underestimate ($ME < 0$) the observed values of $\log K_r$. This bias to overestimate or underestimate rHCC in the sample is better characterized by the mean error [Eq. (20)] in each of the following nine j suction intervals, represented by their limits (in cm): 1.0, 3.2, 10, 32, 100, 320, 1000, 3200, 10000, 20000:

$$ME_j = \sum_{i=1}^{i=N_j} \frac{\left[Y^*(h_{ji}) - Y_o^*(h_{ji})\right]}{N_j}, 1 \le j \le 9 \quad (20)$$

where N_j indicates the number of h_{ji} suctions observed in the j interval, Y* indicates the value calculated by the model from its parameters, and Y_o* indicates the corresponding observed value.

For a set of samples, we will adopt the arithmetic mean of the RMSE values of the samples as a measure of the global quality of fitting of the model. As a global measure of the overestimation and underestimation bias of the rHCC data, we adopted, for each j interval of suction described above, the weighted mean of the ME_j values in the set of samples with weights equal to the N_j values of the samples.

3. Results and discussion

3.1. Evaluation of the model performance

The MGD model will be evaluated with the MVG model [Eq. (1)] as a reference. It will be tested mainly on a global scale of the two databases (UNSODA and Vereecken) using the following three groups of soils in each database: all soils; group A, formed by soils with $RMSE_{MGD} < 0.32$, where $RMSE_{MGD}$ is the RMSE value calculated with Eq. (18) in the evaluation of MGD; group B, formed by soils with $RMSE_{MGD} \ge 0.32$. This standard was established because, as shown below, the rHCC of soils in A is generally well fitted by MGD, giving small errors in all suction intervals tested, as in Figs. 1 and 3, which does not generally happen with soils in B. Graphic representations of rHCC optimized with MGD and MVG are presented for some samples selected from A and B for illustration and the sake of analysis.

3.1.1. UNSODA database

The MVG soil parameters and the RMSE statistics of the model ($RMSE_{MVG}$) for the UNSODA database were obtained by Schaap and Leij (2000) and were courtesy of the first author. Table 1 presents the $RMSE_{MGD}$ and $RMSE_{MVG}$ mean values for the three soil groups mentioned above. It can be seen that the errors decreased from $RMSE_{MVG} = 0.47$ to $RMSE_{MGD} = 0.22$ for the total number of soils from UNSODA (n = 141), a significant reduction of 53%. This reduction was even greater in soil group A (n = 119), where MGD describes the $K_r(h)$ curve with good accuracy, as in this group $RMSE_{MVG} = 0.46$ and $RMSE_{MGD} = 0.18$, a reduction of 61%. In group B (n = 22), the quality of representation of rHCC by MGD is poorer ($RMSE_{MGD} \ge 0.32$ for all soils); yet, the model proposed was more accurate than MVG ($RMSE_{MVG} = 0.54$, $RMSE_{MGD} = 0.47$). Fig. 4 shows the probability distribution functions of RMSE of the three soil groups, making evident the better data fitting of MGD in relation to MVG for any of the groups. We must also point out that soils with a good quality of fitting by MGD (group A) make up 84% of the total of soils from UNSODA, as shown in Table 1. With the inclusion of the MF effects, the model GD fitting errors for all the UNSODA data decreased from $RMSE_{GD} = 0.38$ (as in Table 1 in Ottoni Filho et al., 2019) to $RMSE_{MGD} = 0.22$ (Table 1), a reduction of 42%.

Table 1
RMSE mean errors for the MGD and MVG models for the three soil groups from the two soil databases studied.

Soil Groups	UNSODA database			VEREECKEN database		
	Number of Soils (p ***)	MGD model	MVG model	Number of Soils (p ***)	MGD model	MVG model
All soils	141 (100%)	0.22	0.47	108 (100%)	0.33	0.28
Group A*	119 (84%)	0.18	0.46	66 (61%)	0.22	0.28
Group B**	22 (16%)	0.47	0.54	42 (39%)	0.50	0.30

*Soils with $RMSE_{MGD} < 0.32$; ** soils with $RMSE_{MGD} \ge 0.32$; *** p = percent number of soils.

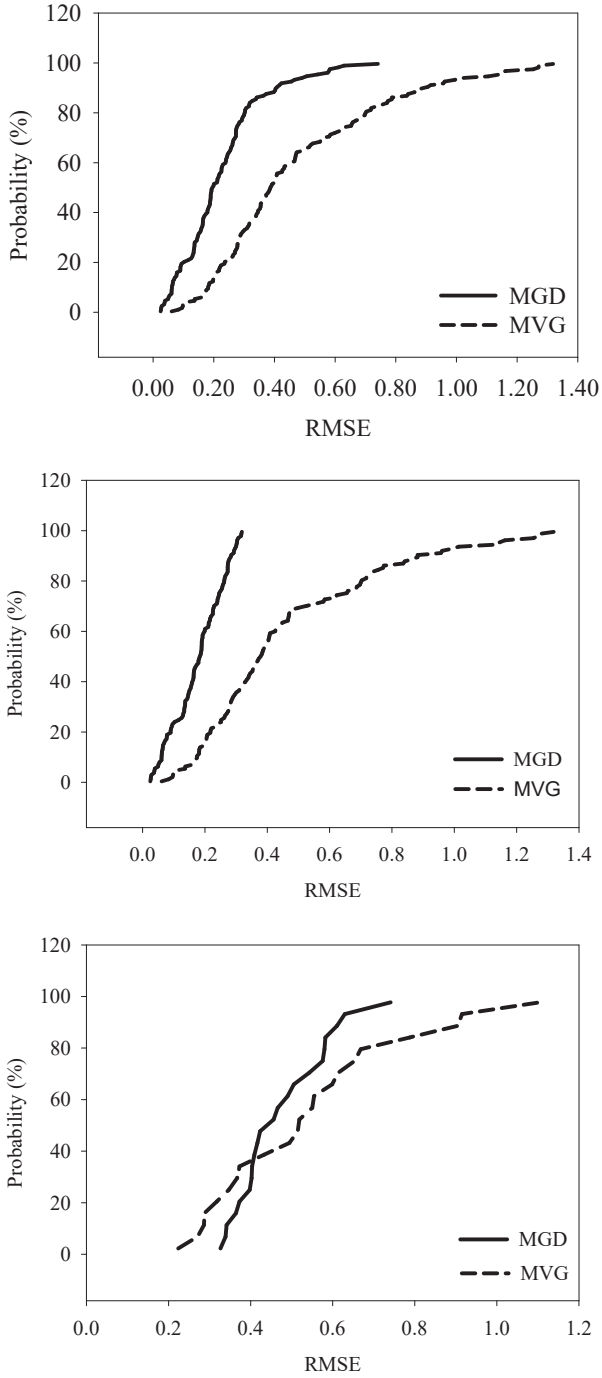

Figure 4. Probability distribution curves of the RMSE values of the three soil groups from the UNSODA database for models MGD and MVG. (a) all soils; (b) soils with $RMSE_{MGD} < 0.32$; (c) soils with $RMSE_{MGD} \ge 0.32$.

Fig. 5 presents the global mean distribution of the sample mean errors, ME_j [Eq. (20)], for MGD and MVG calculated for the nine j suction intervals mentioned in Section 2.4, considering all the UNSODA soils (n = 141). It also shows the number of samples of each interval. This allows evaluating the overestimation (ME > 0) or underestimation (ME < 0) bias in the determination of the measured values of K_r of the two models over the various suction intervals, such as described in Section 2.4. The figure shows a low underestimation and overestimation bias for MGD [$abs(ME_j) \le 0.08$] in the nine suction intervals, with the exception of

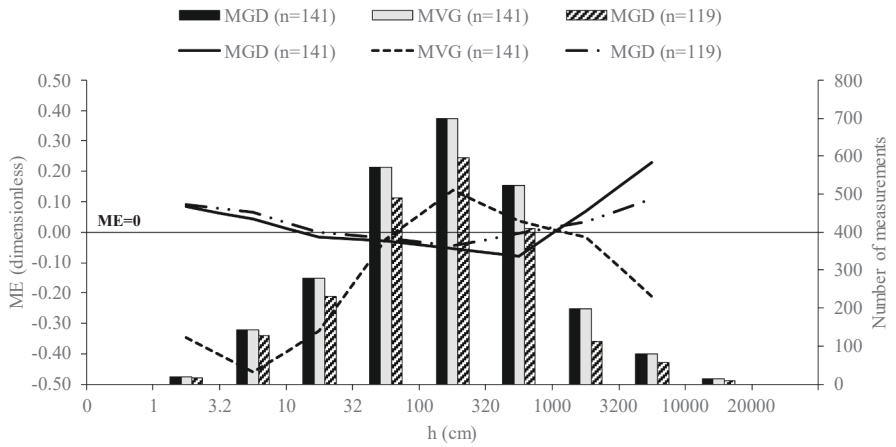

Figure 5. Global mean values of the ME statistics of models MGD and MVG calculated in the nine suction intervals considered (lines), and the number of measurements in each interval (bars). These indicators are taken for the totality of UNSODA database soils (n = 141) and also for the soil group where $RMSE_{MGD} < 0.32$ (n = 119), in this case considering only the MGD model. When the number of soils in the suction interval is small (n < 15), the statistics are not presented.

suctions higher than 3200 cm (log h = X = pF > 3.5), where MGD tends to overestimate the measured values (ME = 0.23). As to MVG, the figure shows a strong bias to underestimate measured rHCC values with suctions lower than 32 cm (pF < 1.5), as already observed by Schaap and van Genuchten (2006) in UNSODA. This is probably due to the limited capacity of MVG to model the MF effects (Durner, 1994). In the highest suction interval (3200 cm < h < 10,000 cm), the MVG underestimation bias repeats (ME = -0.21). Comparing the MGD curve in Fig. 5 (n = 141)

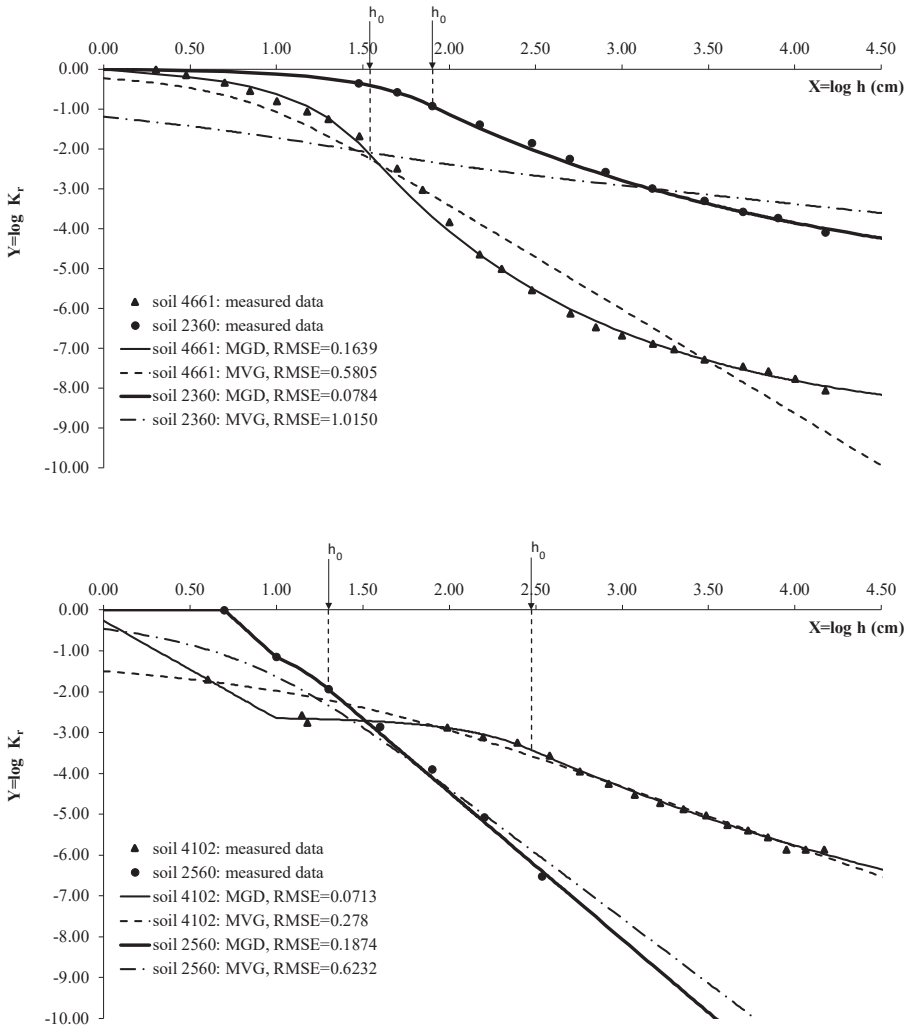

Figure 6. Examples of $K_r(h)$ curves optimized with models MGD and MVG when $RMSE_{MGD} < 0.32$ (group A soils) in the UNSODA database. (a) soils without relevant macropore flow effects: soil 2360 [M = 0, h_a = 0, h_o = 80 cm, λ = 37.5 cm, S_k = 0.927, f(β) = 0.809], soil 4661 [M = 0, h_a = 0, h_o = 35 cm, λ = 7.1 cm, S_k = 2.14, f(β) = 0.712]; (b) soils with relevant macropore flow effects: soil 2560 [M = 0.369, h_a = 5.0 cm, h_o = 20 cm, λ = 5.5 cm, S_k = 1.57, f(β) = 0.998], soil 4102 [M = 2.62, h_a = 0.78 cm, h_o = 300 cm, λ = 161 cm, S_k = 0.807, f(β) = 0.880].

with the corresponding GD curve (n = 153) in Fig. 10 in Ottoni Filho et al. (2019), an improvement can be seen again in the quality of fitting introduced in GD when the MF effects are included by MGD. Interestingly, this improvement occurs both at low (h < 30 cm) and high (h > 1000 cm) suction values.

When only soils with small $RMSE_{MGD}$ errors (group A) are presented in Fig. 5 (n = 119), we notice that the optimization of MGD determines the $K_r(h)$ data with low bias over all the suction intervals tested [abs $(ME_j) \leq 0.11$]. That is, in this case the rHCC modeled by MGD tends to have a good adherence to the experimental dataset, as in Figs 1, 3 and 6. The aim of Fig. 6 is to illustrate the fittings of some soils in group A with MGD and MVG, where MGD usually performs better than MVG, as previously found. Fig. 6a gives examples of cases with parameters M = 0 and $h_a = 0$, that is, soils from group A without relevant MF effects. Note that the experimental points of the two soils in this figure converge asymptotically to the X axis as they get closer to the origin of the coordinate axes (h = 1 cm, $K_r = 1$), which eliminates the possibility of relevant MF. Fig. 6a clearly shows the incapacity of MVG to model rHCC with good adherence to the data when the experimental plot has a tendency of curvature when h is greater than the inflexion point (h_o). This is because MVG imposes a linear relationship to rHCC in the bilogarithm scale at higher suctions. Figs. 3 and 6b illustrate cases where parameter M was optimized with a positive value, therefore, exhibiting MF effects. It can be seen in Fig. 6b that soil 4102, with M = 2.6, presents more intense MF effects than soil 2560, with M = 0.37. The greater impact of the MF flows of the first soil is consistent with its smaller air-entry suction (h_a = 0.78 cm) in relation to soil 2560 (h_a = 5.0 cm), because the smaller the h_a parameter, the greater the diameters and fluxes of the largest pores of the macropore network that sustains MF. The good quality of fitting of soil 4102 with MVG in Fig. 6b ($RMSE_{MVG}$ = 0.28) stands out, but due to a mathematical restriction of MVG [from Eq. (1a), $K_r(h = 0) = K_{ro}$], it is still not possible for $K_r(h = 0)$ to be equal to 1, which is an inconvenience.

In order to evaluate the limitations of optimization of the proposed model, Fig. 7a shows the optimization of cases of poor performance of MGD ($RMSE_{MGD} \geq 0.32$). In Fig. 5 we can see that in the higher suction intervals (3200 cm < h < 10,000 cm), the positive ME error of MGD doubles when soils from group B (n = 22) are added to the 119 soils from group A, that is, when all the soils from UNSODA are considered (n = 141). Therefore, in soils with poorer performance by MGD, the model has a tendency to overestimate the data in intervals with higher suction, as shown in Fig. 7a. Analysis of the experimental plots of log K_r vs. log h of the 22 samples in group B reveals that most soils have a second inflection point (in the interval $h > h_o$) when suctions are close to or greater than h = 1000 cm (X = pF ≈ 3), as pointed out with solid-line circles in the two examples in Fig. 7a. This second inflection systematically creates a relevant disturbance in the MGD optimization, resulting in an overestimation of the K_r data at higher h values. To confirm this disturbance effect, we selected six soils from group B with the greatest $RMSE_{MGD}$ values that also had a double inflection, and reoptimized MGD by eliminating suction values higher than 1000 cm. The result was that the mean $RMSE_{MGD}$ value of the six soils fell sharply from 0.49 (without data elimination) to 0.30 (with data elimination). These second or multiple inflections of the $K_r(h)$ data in the suction interval studied (h < 15,000 cm) may have been due to experimental errors. However, they most probably were caused by hydrodynamic effects introduced by peculiarities in the physical structure of the pore matrix of the soils, such as soils with multimodal pore size distributions (Coppola, 2000; Durner, 1994; Priesack & Durner, 2006). They may also have been caused simply by singular variations in hydraulic complexity of the hydrated pore system due to soil drying and the corresponding increase in the viscous adsorption forces in relation to the capillary forces, which is beyond the scope of our analysis here. All this probably disturbs the simple empirical law expressed in Eq. (3) that gives the fundamentals of MGD. Fig. 7b shows the optimization of MGD and MVG in other two soils from group B to illustrate a second limitation presented by MGD. This limitation is related to the pore structures that do not present MF, but that are sufficiently fine to generate relatively high air-entry suctions (h_a), in the order of 10 cm or more, as indicated by two dashed-line circles in the figure. In this case, without a correction of the Gardner equation [Eq. (3a)] that takes h_a into account, all the K_r calculations close to saturation, as well all the MGD optimization are disturbed, as can be observed in the two examples in Fig. 7b. However, this second limitation of MGD was less frequent in group B than the first one. Likewise, experimental errors in the rHCC data (such as possibly presented by soil 4052 in Fig. 7b in the 1.5 < X < 2 interval) most likely have also interfered with the quality of fitting of the two models.

3.1.2. *Vereecken database*

The soil parameters of MVG [Eq. (1)] for this database were optimized with the RETC program (van Genuchten et al., 1991), using the option "simultaneous fit of θ(h) and K(h) data". No parameter was present in RETC, with the exception of θ_s, which was made equal to the measured value of θ at saturation. The global result with the mean $RMSE_{MGD}$ and $RMSE_{MVG}$ values for all soils, as well as for soils in groups A and B, are given in Table 1. Fig. 8 gives the probability distributions of RMSE values of the two models for the three soil groups. According to Table 1 and Fig. 8a, in the evaluation that considers all the soils from the database, MVG gave a general better fitting (RMSE = 0.28) than the proposed model (RMSE = 0.33), in contrast to what happened with the UNSODA database. However, considering only the 66 soils with good MGD performance (samples with $RMSE_{MGD} < 0.32$), it can be seen that, such as occurred in UNSODA, MGD was generally more efficient than MVG ($RMSE_{MGD}$ = 0.22; $RMSE_{MVG}$ = 0.28), which is confirmed by Fig. 8b. We point out that the soils in group A predominate in the Vereecken database (61% of the soils, according to Table 1), such as occurred in the UNSODA. However, the MGD performance falls sharply when only the soils in group B are considered, since $RMSE_{MGD}$ increased from 0.22 (group A) to 0.50 (group B). In group B, with 42 samples (39% of the total), MVG was far more efficient than MGD, because $RMSE_{MVG}$ = 0.30 (also see Fig. 8c), which justifies the global performance of MVG in the whole database being better than that of MGD.

Analysis of the distribution of the ME_j error in the nine suction intervals (Fig. 9) confirms that, when h > 320 cm suction, the abs(ME_j) values of MGD are, in general, far greater than those of MVG, when all the Vereecken soils are considered. In this case, we see that the errors introduced by MGD can be relevant, both underestimation errors (ME = -0.26 in the interval 320 cm < h < 1000 cm) and overestimation errors (ME = 0.33 in the interval 10000 cm < h < 20000 cm). However, when only soils in group A are considered (graph with n = 66), the optimization of MGD is generally efficient and has a good adherence to the experimental data. This is because, in this case, besides RMSE < 0.32, the ME values also remained low [abs(ME_j) ≤ 0.11] over all the suction intervals tested, such as happened with UNSODA. This confirms that the relevant errors mentioned above in the optimization of MGD were those produced by the soils in group B, such as in UNSODA. The general performance of MVG in the Vereecken database was superior to that in the UNSODA database, as shown in Table 1 and Figs. 8 and 9. This might be justified by the fact that the Vereecken database is regional, while UNSODA is transcontinental. It has to be mentioned that in the Vereecken database MVG maintains, such as occurred in UNSODA, the underestimation bias of K_r data, both in low (h < 10 cm) and high (h > 10,000 cm) suction intervals, as shown in Fig. 9.

Fig. 10 presents cases of good fitting of MGD (group A) with the Vereecken soils in conditions where the model predicts that relevant MF does not exist (M = 0, Fig. 10a) or exists (M > 0, Fig. 10b), and compares them to the MVG fitting. In these cases of group A, as previously said, the performance of MGD tends to be superior to that of MVG, as shown in the figure. When M = 0, we observe again that the K_r data tend to converge to the origin (h = 1 cm, K_r = 0) of the coordinate axes asymptotically, non-abruptly, to the X-axis. We call the attention to a second inflection point in the plot of the data of soil P28_Ap(2)

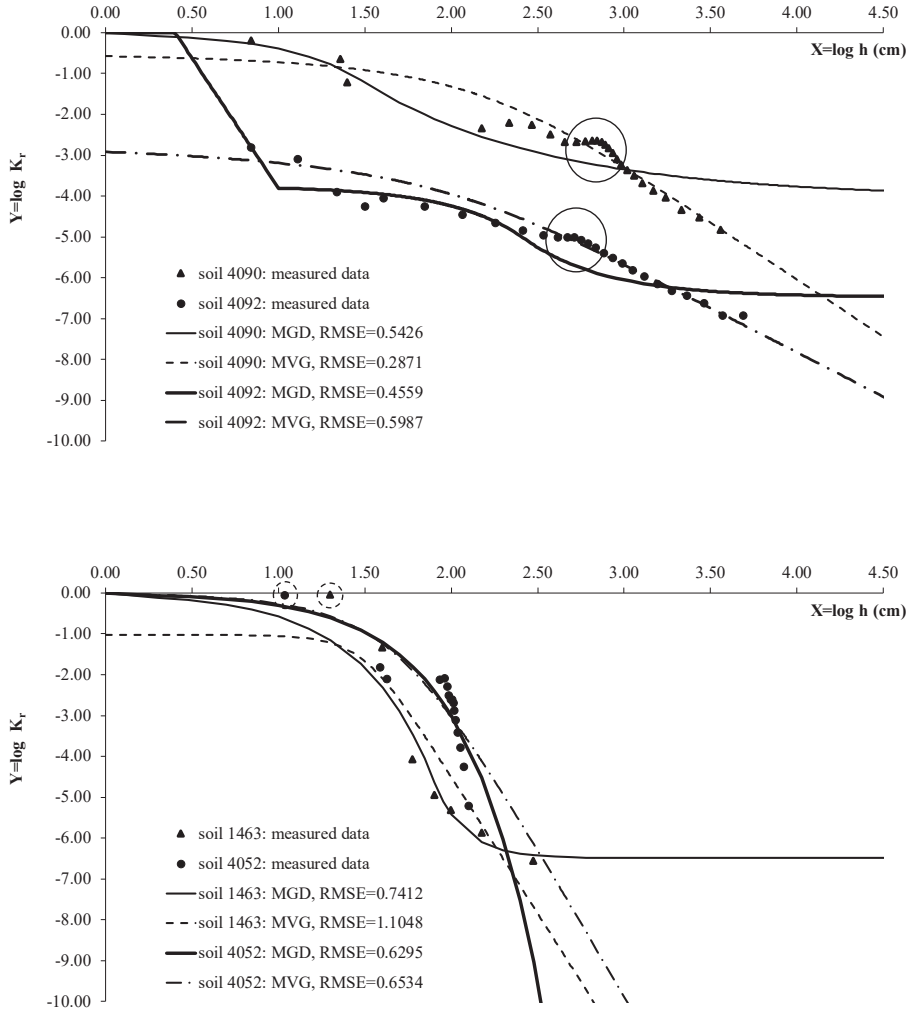

Figure 7. Examples of $K_r(h)$ curves optimized with models MGD and MVG when $RMSE_{MGD} \geq 0.32$ (group B soils) in the UNSODA database. (a) soils with a second inflection point (in the $h > h_o$ branch) of the experimental data of the curve (indicated with a solid-line circle); (b) soils with air-entry suction in the order of 10 cm or more (indicated with a dashed-line circle).

(Fig. 10a), around X = 3.5 (h = 3200 cm), but that did not lead to a high RMSE value for the sample [which would happen if higher h values (X = pF > 4) were tested]. This all indicates a possible loss of efficacy of the proposed model at very high suction levels, such as higher than 15,000 cm, as previously mentioned. In the cases where MGD indicates M > 0 (Fig. 10b), ideally there should be more data with h < 10 cm to allow a more robust fitting of rHCC in these hydrologically relevant intervals of dual permeability close to saturation. The figure exemplifies the greater tendency of MF presented by sample P16_C2(1) (M = 2.6) in relation to sample P28_B2t(1) (M = 1.1).

Fig. 11 illustrates the limitations of MGD in its optimization of the Vereecken database soils from group B ($RMSE_{MGD} \geq 0.32$). Such as happened in UNSODA, the most frequent limitation was probably due to hydraulic/structural peculiarities associated with the presence of a second (or multiple) inflection(s) in the plot of log K_r vs. log h data (Fig. 11a), which usually occurs around the suction of 1000 cm and also above (such as in sample P28_Ap(2) in Fig. 10a). Eliminating the data h > 1000 cm of these peculiar soils of group B and performing a new MGD parameter optimization, a great reduction is observed in the $RMSE_{MGD}$ again in relation to the original value, which, as already mentioned, had happened in the UNSODA database. This confirms that the presence of a second inflection is the main impairment to the MGD fitting in these soils. Fig. 11a exemplifies how the second inflection affects the representation of rHCC by MGD in the highest suction intervals, illustrating the model fitting sensitivity to the presence of these soil hydraulic/structural peculiarities. It is interesting to note that in the Vereecken database, the quality of fitting of MVG was generally less sensitive to the presence of the second inflection than of MGD, as shown in the two samples in Fig. 11a, where MVG showed to be more efficient than MGD. The presence of this second inflection was probably the main reason for the better performance of MVG in relation to MGD in group B soils from the Vereecken database. In soil P31_B2t(2) (Fig. 11a), the MGD curve is not represented at suction values lower than 10 cm due to lack of data in this interval, which did not allow the optimization of parameter h_a. Another less frequent reason than that described above which limited the MGD performance in group B soils (such as happened with the UNSODA soils) was the presence of suction data nearly equal to or higher than 10 cm with the corresponding K_r data practically equal to 1, that is, when the air-entry suction was in the order of h_a = 10 cm or higher, which makes the Gardner exponential equation [Eq. (3a)] ineffective. This happened for soil P26_A/B(1) (Fig. 11b). Experimental inconsistencies of rHCC data (sample P38_Ap(2) in Fig. 11b) certainly also influenced the quality of fitting of the models.

Considering all the soils from the two databases together (249 soils) and using the data in Table 1, we conclude that for the 185 samples of group A, that is, most of the samples, 74% of the total, the proposed model (MGD) generally performed better than the reference model (MVG). In this global set of soils from group A, the mean fitting errors

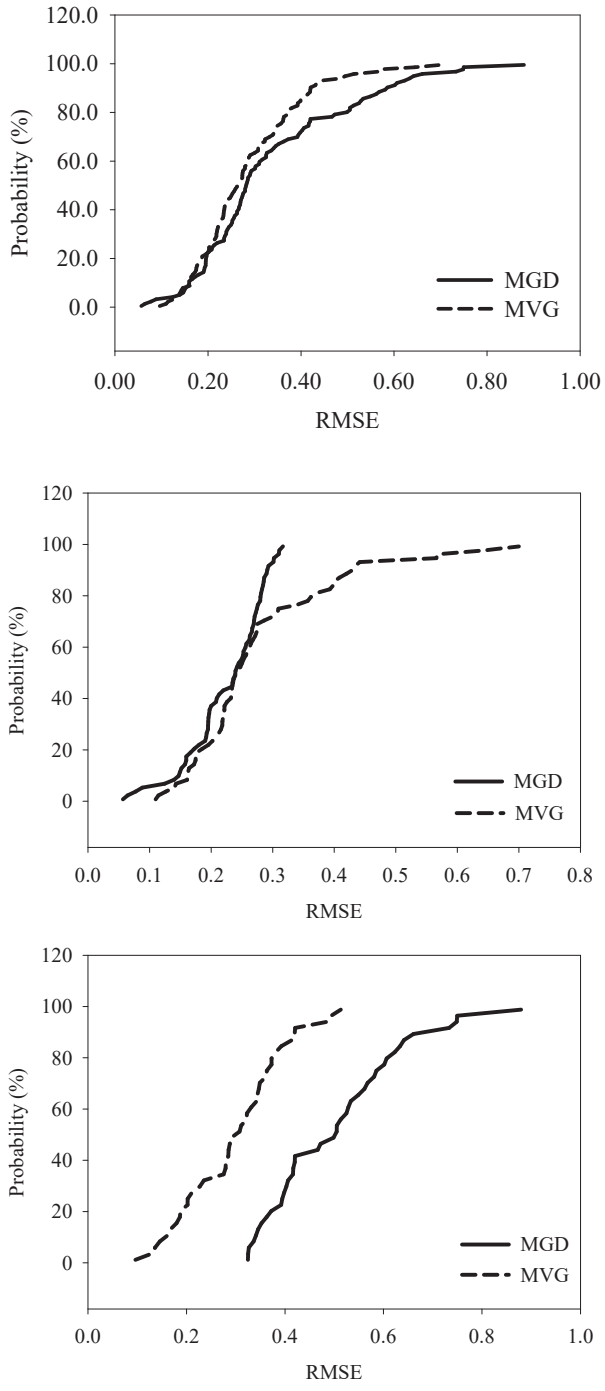

Figure 8. Probability distribution curves of the RMSE values of the three soil groups from the Vereecken database for models MGD and MVG. (a) all soils; (b) soils with $RMSE_{MGD} < 0.32$; (c) soils with $RMSE_{MGD} \geq 0.32$.

were $RMSE_{MGD} = 0.19$ and $RMSE_{MVG} = 0.40$, with thus a great reduction of errors of 53% when MGD was used, in relation to the reference model. The mean quality of fitting of MGD in soils of this group is thus similar to that of the soil presented in Fig. 1, which had $RMSE_{MGD} = 0.16$. In the other soils (group B soils, 26% of the total), when the accuracy of the proposed model deteriorated in relation to that observed for soils in group A, MGD was more accurate than MVG with the UNSODA database and less accurate with the Vereecken database, in general. The mean errors of all the soils from the two databases were $RMSE_{MGD} = 0.27$ and $RMSE_{MVG} = 0.39$.

The global performance of the proposed model can be partially compared to those of the RMSS and FXWJD models analyzed by Rudiyanto et al. (2020), because 211 out of the 232 soil samples they investigated were from the same K(h)-UNSODA database (Schaap & Leij, 2000), from which 141 samples were taken and used in the present study. We can thus say that model MGD was seemingly more accurate than models RMSS and FXWJD in relation to the UNSODA data, since $RMSE_{MGD} = 0.22$ (n = 141, Table 1), $RMSE_{RMSS} = 0.52$ (n = 232) and $RMSE_{FXWJD} = 0.41$ (n = 232), the latter two errors being from Rudiyanto et al. (2020).

3.2. Evaluation of the model parameters

The focus of this section is to present the MGD model parameters as soil hydraulic constants. We will also briefly evaluate the distribution of the values of these parameters in the two databases studied. The analysis will be conducted only for group A soils because, as seen, MGD in general did not represent the reality of the $K_r(h)$ curve adequately for the other soils.

3.2.1. Macropore flow parameters

The macropore flow (MF) exponent, M, and the air-entry suction, h_a, are the two MF parameters of MGD. Constant M is a parameter defined based on two hydrodynamic properties of the soil, K_s and K_{sm}. Conductivity K_{sm} is obtained from K_s and M from Eq. (7). Therefore, both M and h_a are soil hydraulic parameters optimized by the model.

The effective porosity (EP), $EP = \theta_s - \theta_{330}$, where θ_s is the saturated water content and $\theta_{330} = \theta$ (h = 330 cm), is a variable largely used in the prediction of K_s with pedotransfer functions (PTFs) (Abdelbaki, 2021; Ottoni et al., 2019). Considering the definition above, EP is related only to the distribution of the volume of voids in the wet interval (h < 330 cm), and does not reflect the hydrodynamic influence of the macropore network of a soil that has MF, also taking into account that this network normally does not have volumetric relevance in the bulk soil volume (Beven & Germann, 1982; Jarvis, 2007).Therefore, because K_{sm}, the saturated hydraulic conductivity due to matrix flow, does not incorporate the effects of the component of the saturated hydraulic conductivity due to MF, EP is expected to be more correlated to K_{sm} than to K_s in datasets containing some soils that present MF. This is what happens in Figs. 12a and 12b related to the Vereecken database, where the Pearson correlation coefficient presented a large increase from r = 0.559 (K_s vs. EP) to r = 0.816 (K_{sm} vs. EP), respectively. Or in Figs. 12a and 12c, from a different perspective, when r increased from r = 0.559 (K_s vs. EP, all soils) to r = 0.854 (K_s vs. EP, only soils without MF, where M = 0). It would not be possible to construct the scattergrams of Figs. 12b and 12c, more correlated to the EP than the scattergram of Fig. 12a, as expected, without the determination of M. This corroborates the statement that parameter M has a physical meaning. From the example above, we conclude that M can be used in the development of more efficient PTFs of K_s by filtering the influence of MF on the value of K_s, that is, by determining K_{sm}. This would meet a demand in the literature for the prediction of K_s with PTFs, which reports the inconvenience of the increase of the variance in the K_s prediction due to hydrodynamic effects of the macropore space of the soils (Ottoni et al., 2019; Weynants et al., 2009; Zhang et al., 2019). It was not possible to study a case similar to that presented above using the UNSODA database, because the measured value of θ_s used in EP is not available in this database. The value of θ_{330} used to determine EP in Fig. 12 was calculated with Eqs. (1b) and (1c) from the parameters of these equations.

Table 2 gives an approximate description of the distribution of the values of M (M > 0) and h_a in the two databases. Out of the 119 soils from UNSODA in group A, only 42 soils presented MF effects (M > 0), while the corresponding numbers in the Vereecken database were 66 and 37. We speculate that the smaller proportion of soils with MF in the first database was probably due to the fact that UNSODA contains only soils selected from the literature, while the Vereecken database is

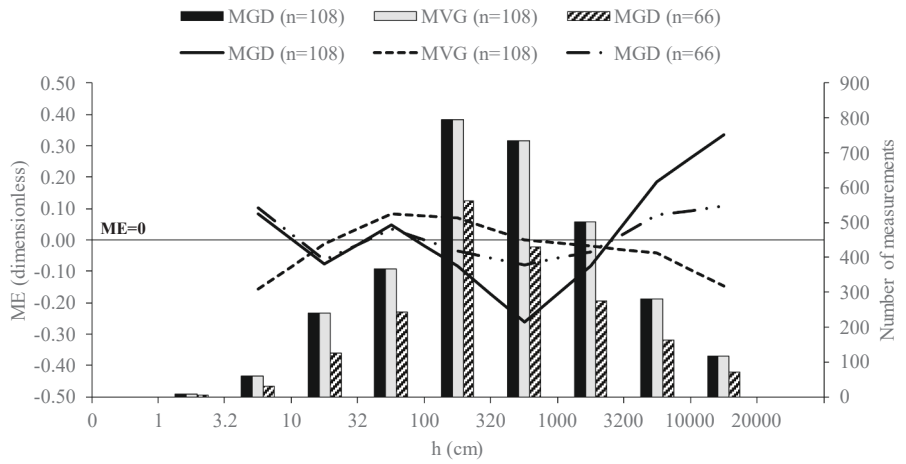

Figure 9. Global mean values of the ME statistics of models MGD and MVG calculated in the nine suction intervals considered (lines), and the number of measurements in each interval (bars). These indicators are taken for the totality of the Vereecken database soils (n = 108) and also for the soil group where $RMSE_{MGD} < 0.32$ (n = 66), in this case considering only the MGD model. When the number of soils in the suction interval is small (n < 15), the statistics are not presented.

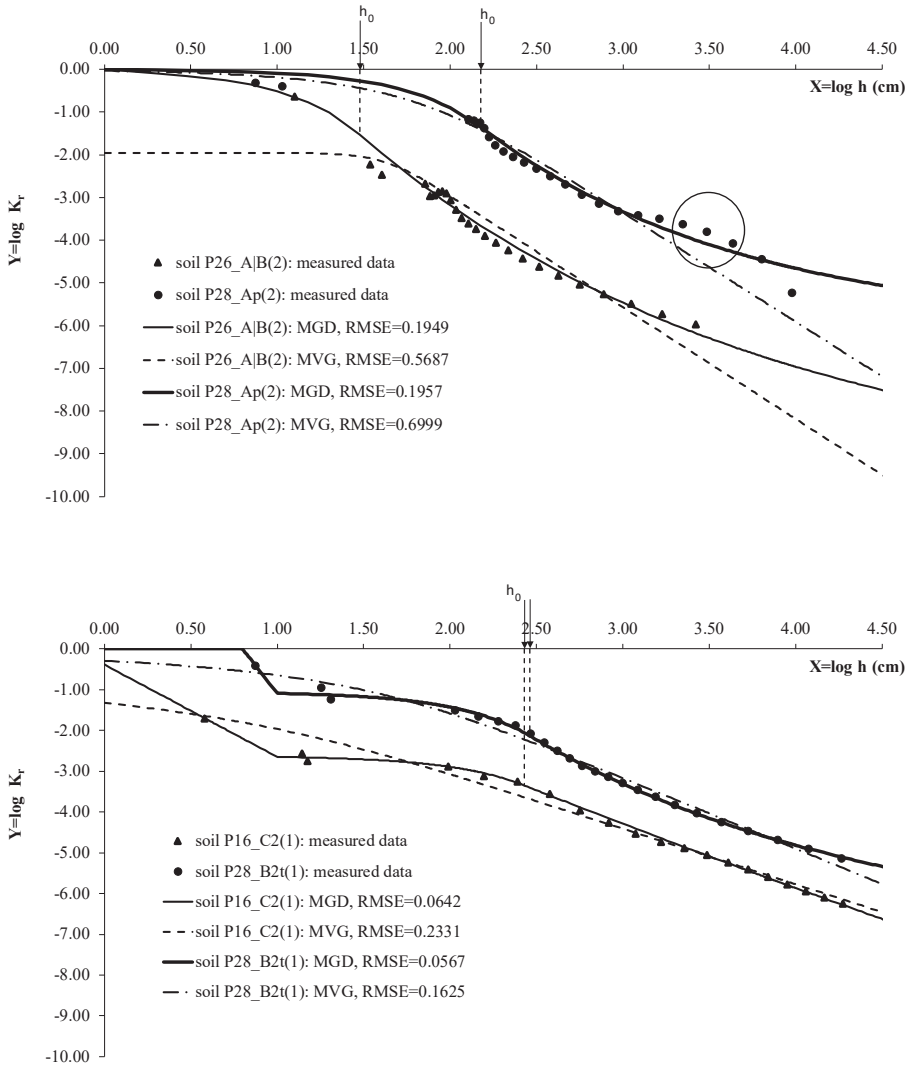

Figure 10. Examples of $K_r(h)$ curves optimized with models MGD and MVG when $RMSE_{GDm} < 0.32$ (group A soils) in the Vereecken database. (a) soils without relevant macropore flow; (b) soils with relevant macropore flow. The solid-line circle on the experimental plot of soil P28_Ap(2) indicates the presence of a second inflection of the data at suction values higher than the transition suction, h_o (main inflection of the curve).

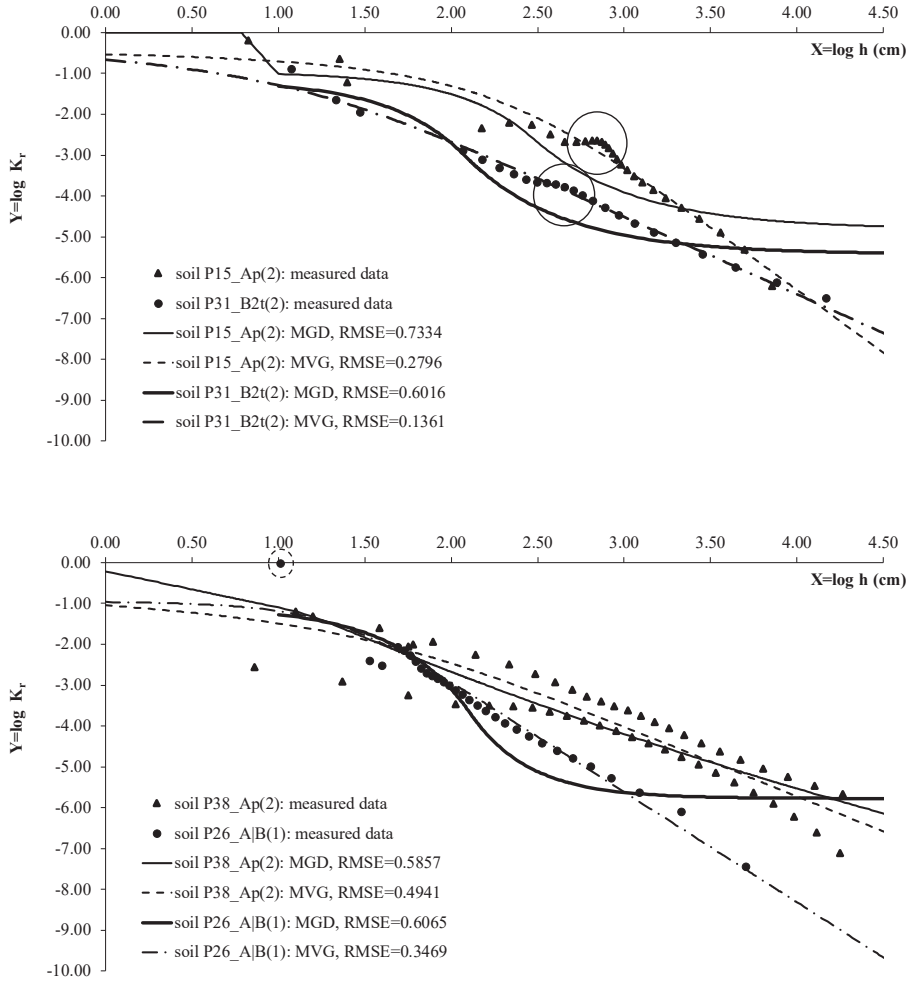

Figure 11. Examples of $K_r(h)$ curves optimized with models MGD and MVG when $RMSE_{MGD} \geq 0.32$ (group B soils) in the Vereecken database. (a) soils with a second inflection point (in the $h > h_o$ branch) of the experimental data of the curve (indicated with a solid-line circle); (b) soils with air-entry suction in the order of 10 cm or more (indicated with a dashed-line circle).

formed by the main soils of a specific region (Northern Belgium), and, therefore is influenced by regional pedologic factors. However, Table 2 reveals that despite the distinct pedology of the two databases, the statistics of their distributions of M values were relatively close, with differences always smaller than 26%, with the exception of X_{10} (X_{10} defined in the footnote of Table 2). The mean values of M were around 1.5, with coefficients of variation close to 55% (which makes M a property of great variation, according to Warrick, 1998). Therefore, by Eq. (7), $K_s/K_{sm} = 10^{1.5} = 32$, as an approximate mean, confirming the relevance of the MF phenomenon and of the M parameter through the large value of this fraction. Low values (X_{10}) of M were close to or smaller than 0.65, while the high values (X_{90}) were close to or>3.0. We will not analyze the distributions of h_a due to the small number of samples where this parameter was optimized, and also because various values of h_a were from samples with only one K_r measurement in the interval $h < 10$ cm, which reduces the representativity of the determination of this parameter.

3.2.2. *Matrix flow parameters*

S_k, the conductive depletion index, is a multiplicative constant of function $Y^* = \log[K_r(h)]$ that describes rHCC determined by MGD. This function is represented by Eqs. (15c) ($M > 0$, $h \geq 10$ cm) or (16) ($M = 0$, $h \geq 0$) that model Y^* in suction intervals where only the matrix flow (mF) occurs. In this way, because S_k influences the logarithmic depletion of rHCC directly, it can be considered to be a physical quality index of the soil: the greater S_k, the more the hydraulic conductivity decreases with the increase in h. In agreement with this fact, due to Eqs. (5) and (12), S_k is also proportional to the absolute value of the dY^*/dX derivative of the bilogarithmic representation of rHCC at its inflection point, h_o. From Eq. (13), coincidently, $S_k = -Y_o^* - M$, where Y_o^* is the value of Y^* at h_o (Fig. 3). Therefore, both S_k and h_o, the transition suction, are physical parameters of great impact on rHCC and, therefore, on the hydrodynamic behavior of soils when rHCC is accurately modeled by MGD. A result consistent with this statement is the fact that parameter λ, the macroscopic capillary length (the inverse of the sorptive number of the infiltration theory), can be determined only from S_k and h_o [Eq. (6)]. According to MGD [Eq. (3a)], as an mF soil parameter, only λ exerts an influence on K_r in wetter matrix flows, with $h < h_o$. These flows are much affected by capillary effects, such as are the infiltration flows without MF effect, when the soil sorptivity depends on λ and K_s (Philips, 1957; Vandervaere, 2002; White & Sully, 1987) and the infiltrometry/permeametry can be applied in the in situ determination of these two variables, as already mentioned.

A last mF parameter in MGD is the β constant, the conductive depletion coefficient. While λ influences the matrix flows when $h < h_o$, its equivalent β only does so when $h > h_o$ [Eq. (3b)]. In the latter case ($h > h_o$), the relative hydraulic conductivity due to mF, $Y(h) = \log K_{rm}$, is calculated with Eq. (16): $Y(h) = -S_k.d_\beta(g)$, $g = h/h_o$, where $d_\beta(g)$ is the depletion function given by Eq. (4b). This confirms that the hydraulics of less wet matrix flows ($h > h_o$) is more complex to describe than that of

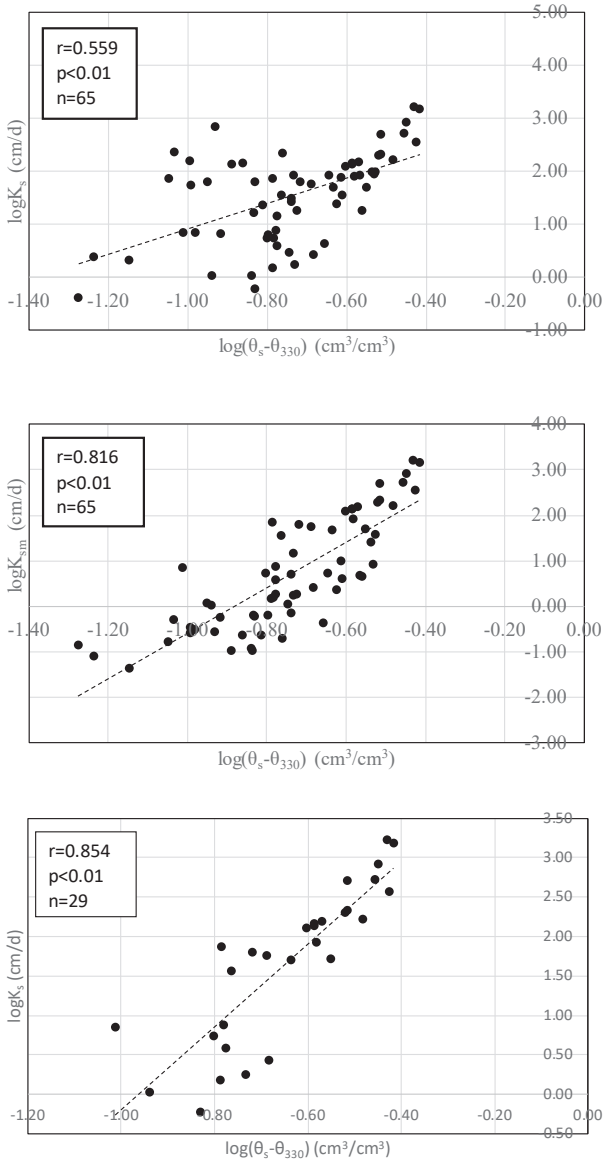

Figure 12. Scattergrams of the saturated hydraulic conductivity (K_s) and the saturated hydraulic conductivity due to matrix flow (K_{sm}) versus the effective porosity (EP) taking group A soils ($RMSE_{MGD} < 0.32$) from the Vereecken database into account. (a) K_s vs. EP (n = 65); (b) K_{sm} vs. EP (n = 65); (c) K_s vs. EP (soils with M = 0, n = 29). The r value is the Pearson correlation coefficient.

the infiltration flows mentioned above, because, in the former, K_r is influenced by h_o, S_k and β, while in the infiltration flows, only λ exerts an influence on K_r. Flows with $h > h_o$ possibly predominate in wetted soil profiles about one to three days after infiltration has ended. Therefore, while classical infiltrometry/permeametry allow the in situ determination of parameter λ, they will not be capable of determining the other mF parameters. A new in situ methodology needs to be conceived based on the measurement of the flows not so close to saturation ($h > h_o$) that occur at some time after the infiltration. Another relevant fact, as already mentioned in section 2.1, is that f(β), the linearization fraction, calculated from β, must be seen as a shape parameter of rHCC, clearly identifiable in Fig. 2, defining the curvature of Y*(log h) at its main inflection, h_o. Ottoni Filho et al. (2019) justified why it is desirable to use f(β) instead of β as a shape parameter of rHCC.

Considering the last two paragraphs, we conclude that all three mF parameters (h_o,S_k, β) and the two MF parameters (M, h_a) depend mainly on the experimental data of the Y*(log h) curve for h data smaller than the transition suction (h_o), and also for h data not much greater than h_o, but sufficiently great to allow the identification of this main inflection of the curve and the curvature of Y*(log h) at the inflection. This is relevant due to the experimental difficulties to obtain rHCC data at high suctions.

As to the distribution of the mF parameter values, Table 2 suggests that the distribution of the S_k index is very similar in the UNSODA and Vereecken databases, with a maximum difference of 20% between the corresponding statistics, such as, in general, also happened with the M parameter. The mean values of S_k were around 1.35, while the low values (X_{10}) were close to or smaller than 0.75, and the high values (X_{90}), close to or>2.0, with the extreme data of $S_k = 0.50$ and $S_k = 3.0$ well characterized. An example of soil with median S_k is sample P28_Ap (2), which has $S_k = 1.35$ (Fig. 10a), while a low S_k of 0.727 was obtained for sample P16_C2(1) (Fig. 10b) and a high S_k of 2.14, for soil 4661 (Fig. 6a). Another mF parameter that characterizes, with positive correlation, the depletion of the hydraulic conductivity in the less wet interval $h > h_o$ is constant f(β) (Fig. 2). This parameter also presented very close corresponding mean, median and high values for the two databases (differences smaller than 16%), with a greater difference for the coefficient of variation and X_{10}, according to Table 2. Median values of f(β) were around 0.75 [soil 4661 in Fig. 6a, with f(β) = 0.712], while high values occurred at the highest limit f(β) = 1 (soil 2560 in Fig. 6b, with f(β) = 0.998). A well-represented minimum value of f(β) was 0.13 (there were five cases in UNSODA with f(β) < 0.10, but from samples with scarce $h > h_o$ data). A relatively low value of f(β) = 0.48 is represented in Fig. 12 by Ottoni Filho et al. (2019). It stands out that the above-mentioned soil 4661 is the same soil illustrated in Figs. 1 and 2, with a rather curvilinear behavior of rHCC in the $h > h_o$ interval. As its f(β) parameter has a value close to the mean and median of the distribution of f(β) in the two databases, we can infer that the cited curvilinear behavior of rHCC of the soil of Figs. 1 and 2 is usual. This points to a limitation of the MVG model in describing rHCCs, since MVG can only produce linear forms of the bilogarithm representation of rHCC in its $h > h_o$ interval. According to Table 2 and in contrast to what happened in

Table 2
Statistics of the distribution of the values of the parameters of model MGD in the two studied databases considering only the soils from group A ($RMSE_{MGD} < 0.32$).

Statistics	MGD Parameter									
	UNSODA database					VEREECKEN database				
	h_o(cm)	λ(cm)	S_k(-)	f(β) (-)	$M > 0$(-)	h_0(cm)	λ(cm)	S_k(-)	f(β) (-)	$M > 0$(-)
mean	70.5	23.8	1.54	0.66	1.62	119	47.2	1.36	0.78	1.48
CV(%)*	106	129	41	39	52	73	92	47	25	58
X_{10}**	10	4.6	0.81	0.33	0.78	25	7.7	0.68	0.49	0.51
median	40.0	11.6	1.40	0.68	1.41	110	28.8	1.29	0.79	1.12
X_{90}***	190	79.4	2.50	1.00	2.99	270	120	2.09	1.00	2.86
Number of samples	117	119	117	117	42	66	66	66	66	37

*Coefficient of variation; **value which exceeds at 10% probability; ***value which exceeds at 90% probability.

relation to S_k and f(β), the distributions of the values of the other two mF parameters (λ and h_o) differed greatly between the two databases, with values λ and h_o generally greater in the Vereecken database than in UNSODA. This may be due to the hydraulic features of the regional soils from the Vereecken database. λ and h_o also varied much more in the two databases than S_k and f(β), with coefficients of variation between 73% and 129% (Table 2), therefore being characterized as high variation parameters, according to Warrick (1998). While the values of h_o varied in the wet suction interval [10 cm, 300 cm], λ fell within [2.0 cm, 161 cm], which is consistent with the literature on infiltration (Communar & Friedman, 2014; Reynolds, 2016; White & Sully, 1987). The corresponding mean (23.8 cm, 47.2 cm) and median (11.6 cm, 28.8 cm) values of λ differed greatly from each other, both in the UNSODA and Vereecken databases, respectively. Soil P16_C2(1) (Fig. 10b) had an extremely low matrix flow depletion of K_r in the $h < h_o$ interval, with $\lambda = 161$ cm [the greater λ, the less K_r decreases with h, according to Eq. (3a)], while soil 4661 (Fig. 6a) is an example of relatively high matrix flow depletion of K_r in the $h < h_o$ interval, with $\lambda = 7.09$ cm. The mean and median values of h_o were 70.5 cm and 40.0 cm, respectively, in the UNSODA database, and 119 cm and 110 cm, in the Vereecken database.

As the four mF parameters of MGD were identified above as hydraulic constants of the soil, it would be desirable to infer, in a preliminary analysis, their correlation with soil properties that are easier to determine, the so-called predictor properties, in order to verify the possibility of determination of λ, h_o, S_k and f(β) using PTFs. We consider as predictor variables in this preliminary study the three textural fractions (S, Si, C – sand, silt, clay percentages), the bulk density (BD) and the θ_{330} value (calculated as in section 3.2.1). The latter will be called arbitrarily as the structural predictor and the first four as the matrix predictors. Table 3 contains the Pearson correlation coefficients (r) of the mF parameters in relation to a grouping (linear combination) of the four matrix predictors and to the structural predictor in the two databases. The r values are not informed in the Vereecken database in relation to the matrix predictors because the data on these predictors were not available. We can conclude that UNSODA presented a significant correlation between the mF parameters [with the exception of f(β)] and the matrix predictors, even though not a strong one. A possible explanation for the lack of correlation between f(β) and the matrix predictors is that f(β) is the only mF parameter entirely dependent on the hydrodynamic characteristics of the finer and more complex, less capillary, hydrated pore space, corresponding to the values of $h > h_o$. It is worth noting that in the Vereecken database, all four mF parameters correlated far better ($0.46 < r < 0.73$) with structural predictor θ_{330}, which is indicative that WRC data may generate efficient predictors of the hydraulic conductivity curve. Now, in the UNSODA database, we can see that the only parameter that correlated with θ_{330} was S_k. We speculate that this poor correlation of mF parameters with the structural predictor may be due to the great diversity of pore structures in the selected international soils from UNSODA, which possibly did not happen with the regional soils from the Vereecken database.

4. Conclusion

The Gardner Dual (GD) model of representation of the relative hydraulic conductivity curve (rHCC), $Y^* = \log[K_r(h)]$, proposed by Ottoni Filho et al. (2019) was extended in this study to include the macropore flow (MF) effects close to saturation. This modification of GD is necessary, since hydraulic and hydrologic effects resulting from the wetting and drainage of soils that present MF are common and relevant in nature and in engineering studies. The new model was called Modified Gardner Dual (MGD) model. It was based on the assumption that the MF effects are relevant only if suction h (a positive number) is smaller than 10 cm. In this $h < 10$ cm range, $K_r(h)$ was presumed to follow the Jarvis (2008) model. From $h > 10$ cm on, we admitted that only the matrix flow (mF) effects were important and that $K_r(h)$ must continue varying according to the GD model. This implied that $Y^*(h)$ could be calculated using very simple analytical expressions [Eq. (15) — if the MF effects are relevant, or Eq. (16), if they are not relevant], and that the coordinates (h_o, Y^*_o) of the main inflection point of the bilogarithmic representation of rHCC were important hydraulic constants of the soil, according to MGD. Parameter h_o was called transition suction and constant Y^*_o is calculated with the expression: $Y^*_o = -(M + S_k)$ [Eq. (13)], where M and S_k are other two positive hydraulic parameters of MGD: the first one (M), called macropore flow exponent, represents the relationship between saturated hydraulic conductivity of the soil and saturated hydraulic conductivity due to mF [Eq. (7)]; the second one (S_k), called conductive depletion index, represents the absolute value of the $dY^*/\ln(h)$ derivative at $h = h_o$ [Eq. (5)]. When M is optimized with a null value, the MGD model indicates that MF effects do not exist, and the opposite when M is positive. Additionally, when $M = 0$, obviously S_k is the absolute value of $Y^*(h_o)$ itself at the inflection of rHCC. It has been demonstrated that the macroscopic capillary length, λ, a parameter acknowledged in the infiltration literature, can be calculated from h_o and S_k alone [Eq. (6)]. Another soil hydraulic parameter of MGD is the β constant, called the conductive depletion coefficient. It is the rHCC depletion constant of the interval $h > h_o$ [Eq. (3b)], corresponding to λ in the depletion of the interval $h < h_o$ [Eq. (3a)], taking into consideration that Eqs. (3a) and (3b) are the basic exponential expressions that define the matrix depletion of $K_r(h)$ in MGD. It is demonstrated that as a soil value, it is more practical and elucidative to consider parameter f(β) (calculated from β) than β. Constant f(β) ($0 < f(\beta) < 1$), called the linearization fraction, must be seen as a shape parameter easily identifiable in rHCC (Fig. 2), defining the curvature of $Y^*(\log h)$ at h_o (for $h > h_o$). The last soil parameter of MGD is the air-entry suction, h_a, a constant with a known physical meaning. Therefore, all the five parameters of MGD [h_o, S_k, f(β), M, h_a] are soil constants with hydraulic meanings, clearly related to the behavior of rHCC (Figs. 2 and 3).

The proposed model was evaluated taking the Mualem-van Genuchten (MVG) model with the flexible parameterization of Eq. (1) as a reference. The evaluation was performed using two databases (UNSODA and Vereecken), the former, international and the latter, regional, totaling 249 soils. Only suction data close to or smaller than 15,000 cm were used in the evaluation, as we supposed that the analytical simplicity of MGD would make it difficult for this model to be efficient at

Table 3
Pearson correlation coefficients between the matrix flow parameters of the MGD model and the matrix and structural predictors.

Predictors	MGD parameter							
	UNSODA database				VEREECKEN database			
	h_0(cm)	λ(cm)	S_k	f(β)	h_0(cm)	λ(cm)	S_k	f(β)
linear combination of S, Si, C, BD (matrix predictor)	0.304 (Yes*)	0.349 (Yes)	0.354 (Yes)	0.090 (No)	***	—	—	—
θ_{330}(structural predictor)	0.004 (No**)	0.130 (No)	0.315 (Yes)	0.059 (No)	0.462 (Yes)	0.661 (Yes)	0.729 (Yes)	0.515 (Yes)
Number of samples	117	119	117	117	66	66	66	66

*significant correlation ($p < 0.01$); **non-significant correlation ($p > 0.16$); *** predictor not available.

extremely high suctions. The RMSE [Eq. (18)] statistics was the main measure used to infer the fitting errors of the log $K_r(h)$ functions set forth by the models for each sample. For 74% of the samples, with soils from the two databases, MGD gave better results than MVG. In this subset of samples (group A), MGD was 53% globally more efficient than MVG, a significant result, as, on average, $RMSE_{MVG} = 0.40$ and $RMSE_{MGD} = 0.19$, with $RMSE_{MGD} < 0.32$ in any sample. Another important result is that in group A the experimental data generally had good adherence to the rHCC optimized with MGD over the whole suction interval, as seen in Fig. 1. However, in the remaining 26% of the samples (group B) the quality of fitting by the proposed model decreased; MGD remained more efficient than MVG in UNSODA, but less efficient in Vereecken. Considering the 249 soils, $RMSE_{MGD} = 0.27$ and $RMSE_{MVG} = 0.39$ on average. Analysis of the data plot (log h, log K_r) of samples from group B shows that the two main causes of loss of accuracy of MGD were, in decreasing order of frequency: a) the presence of at least a second point of inflection in addition to h_o in the data plot, which might characterize a structural and/or hydraulic singularity in the hydrated pore system, foreign to the model (this second inflection generally has $h > 500$ cm, more commonly being around or higher than $h = 1000$ cm); b) the presence of suction data very close to or higher than $h = 10$ cm with a corresponding $K_r \approx 1.0$, which contradicts the hypothesis of MGD that $h_a < 10$ cm, that is, characterizing samples with soil air-entry suction around 10 cm or greater. Therefore, with the exception of the two limitations above, besides being simple and parameterizable with constants with clear hydraulic meaning, the proposed model is expected to be an advantageous option for the representation of $K_r(h)$. The approximate distributions of the values of these constants in the two databases have also been made available in this study.

All the five parameters of MGD are dependent on the behavior of the optimized $K_r(h)$ curve from saturation up to h values not much larger than the transition suction, h_o (but sufficiently large enough to allow the clear identification of the curvature of bilogarithmic rHCC close to h_o). Thus, as in general $h_o \leq 300$ cm, another advantage in using MGD is that its parameters can be obtained using suction data not necessarily very high, like those smaller than 1000 cm.

CRediT authorship contribution statement

Theophilo Benedicto Ottoni Filho: Conceptualization, Methodology, Software, Validation, Visualization, Supervision. **Anderson Rodrigues Caetano:** Software, Validation, Visualization. **Marta Vasconcelos Ottoni:** Software, Validation, Visualization, Project administration.

Declaration of Competing Interest

The authors declare that they have no known competing financial interests or personal relationships that could have appeared to influence the work reported in this paper.

Data availability

The data reference is described in the manuscript

Appendix A. Supplementary material

Supplementary data to this article can be found online at https://doi.org/10.1016/j.hydroa.2023.100155.

References

Abdelbaki, A.M., 2021. Selecting the most suitable pedotransfer functions for estimating saturated hydraulic conductivity according to the available soil inputs. Ain Shams Engineering Journal. 12 (3), 2603–2615.

Ankeny, M.D., Ahmed, M., Kaspar, T.C., Horton, R., 1991. Simple field method for determining unsaturated hydraulic conductivity. Soil Science Society of America Journal 55, 467–470.

Assouline, S., Or, D., 2013. Conceptual and parametric representation of soil hydraulic properties: A review. Vadose Zone Journal 12 (4), 1–20. https://doi.org/10.2136/vjz2013.07.0121.

Beven, K., Germann, P., 1982. Macropores and water flow in soils. Water Resources Research 18 (5), 1311–1325.

Beven, K., Germann, P., 2013. Macropores and water flow in soils revisited. Water Resources Research 49, 3071–3092. https://doi.org/10.1002/wrcr.20156.

Communar, G., Friedman, S.P., 2014. Determination of soil hydraulic parameters with cyclic irrigation tests. Vadose Zone Journal 13 (4), 1–12. https://doi.org/10.2136/vzj2013.09.0168.

Coppola, A., 2000. Unimodal and bimodal descriptions of hydraulic properties for aggregated soils. Soil Science Society of America Journal 64 (4), 1252–1262.

Dexter, A.R., 2004. Soil physical quality. Part I. Theory, effects of soil texture, density, and organic matter, and effects on root growth. Geoderma 120 (3-4), 201–214.

Durner, W., 1994. Hydraulic conductivity estimation for soils with heterogeneous pore structure. Water Resources Research 30 (2), 211–223.

Gardner, W.R., 1958. Some steady-state solutions of the unsaturated moisture flow equation with application to evaporation from a water table. Soil Science 85 (4), 228–232.

Gerke, H.H., Germann, P., Nieber, J., 2010. Preferential and unstable flow: From the pore to the catchment scale. Vadose Zone Journal 9, 207–212. https://doi.org/10.2136/vzj2010.0059.

Gerke, H.H., Dusek, J., Vogel, T., 2013. Solute mass transfer effects in two-dimensional dual-permeability modeling of bromide leaching from a tile-drained field. Vadose Zone Journal 12 (2), 1–21. https://doi.org/10.2136/vzj2012.0091.

Gerke, H.H., van Genuchten, M.T., 1993. A dual-porosity model for simulating the preferential movement of water and solutes in structured porous media. Water Resources Research 29, 305–319. https://doi.org/10.1029/92WR02339.

Jarvis, N.J., 2007. Review of non-equilibrium water flow and solute transport in soil macropores: Principles, controlling factors and consequences for water quality. Eu. J. Soil Sci. 58, 523–546. https://doi.org/10.1111/j.1365-2389.2007.00915.x.

Jarvis, N., 2008. Near-saturated hydraulic properties of macroporous soils. Vadose Zone Journal 7 (4), 1302–1310.

Jarvis, N., Koestel, J., Larsbo, M., 2016. Understanding preferential flow in the vadose zone: Recent advances and future prospects. Vadose Zone Journal 15 (12), 1–11. https://doi.org/10.2136/vzj2016.09.0075.

Jarvis, N.J., Messing, I., 1995. Near-saturated hydraulic conductivity in soils of contrasting texture as measured by tension infiltrometers. Soil Science Society of America Journal 59, 27–34.

Lassabatere, L., Yilmaz, D., Peyrard, X., Peyneau, P.E., Lenoir, T., Simunek, J., Angulo-Jaramillo, R., 2014. New analytical model for cumulative infiltration into dual-permeability soils. Vadose Zone Journal 13 (12), 1–15. https://doi.org/10.2136/vzj2013.10.0181.

Lebeau, M., Konrad, J.M., 2010. A new capillary and thin film flow model for predicting the hydraulic conductivity of unsaturated porous media. Water Resources Research 46, W12554. https://doi.org/10.1029/2010WR009092.

F.J. Leij W.J. Alves M.T. van Genuchten J.P. Williams The UNSODA unsaturated soil hydraulic database, version 1.0, EPA report EPA/600/R-96/095, EPA National Risk Management Laboratory 1996 Cincinnati, OH.

Leij, F.J., Russell, W.B., Lesch, S.M., 1997. Closed-form expressions for water retention and conductivity data. Ground Water 35 (5), 848–858.

Nemes, A., Schaap, M.G., Leij, F.J., Wösten, J.H.M., 2001. Description of the unsaturated soil hydraulic database UNSODA version 2.0. Journal of Hydrology 251 (3-4), 151–162.

Ottoni Filho, T.B., Alvarez, M.G.L., Ottoni, M.V., Amorim, A.B.B.D., 2019. Extension of the Gardner exponential equation to represent the hydraulic conductivity curve. J. Hydrol. Hydromech 67 (4), 359–371. https://doi.org/10.2478/johh-2019-0015.

Ottoni, M.V., Ottoni Filho, T.B., Lopes-Assad, M.L.R.C., Rotunno Filho, O.C., 2019. Pedotranfer functions for saturated hydraulic conductivity using a database with temperate and tropical soils. Journal of Hydrology 575, 1345–1358. https://doi.org/10.1016/S0016-7061(98)00132-3.

Peters, A., 2013. Simple consistent models for water retention and hydraulic conductivity in the complete moisture range. Water Resources Research 49, 6765–6780. https://doi.org/10.1002/wrcr.20548.

Peters, A., Durner, W., 2008. A simple model for describing hydraulic conductivity in unsaturated porous media accounting for film and capillary flow. Water Resources Research 44, W11417. https://doi.org/10.1029/2008WR007136.

Peters, A., Hohenbrink, T.L., van Iden, S.C., Genuchten, M.Th., Durner, W., 2023. Prediction of the absolute hydraulic conductivity function from soil water retention data. Hydrol. Earth Syst. Sci. 27, 1565–1582. https://doi.org/10.5194/hess-27-1565-2023.

Philip, J.R., 1957. The theory of infiltration, 4, Sorptivity and algebraic infiltration equations. Soil Science 84 (3), 257–264.

Philip, J.R., 1969. Theory of infiltration. Advances in Hydroscience 5, 215–296. https://doi.org/10.1016/B978-1-4831-9936-8.50010-6.

Priesack, E., Durner, W., 2006. Closed-form expression for the multi-modal unsaturated conductivity function. Vadose Zone Journal 5 (1), 121–124.

Raats, P.A.C., Gardner, W.R., 1971. Comparison of empirical relationships between pressure head and hydraulic conductivity and some observations on radially symmetric flow. Water Resources Research 7 (4), 921–928.

Reynolds, W.D., 2008a. Saturated hydraulic properties: Ring infiltrometer. In: Carter, M. R., Gregorich, E.G. (Eds.), Soil Sampling and Methods of Analysis, 2nd ed. CRC Press, Boca Raton, FL, pp. 1043–1056.

Reynolds, W.D., 2008b. Unsaturated hydraulic properties: Field tension infiltrometer. In: Carter, M.R., Gregorich, E.G. (Eds.), Soil Sampling and Methods of Analysis, 2nd ed. CRC Press, Boca Raton, FL, pp. 1107–1127.
Reynolds, W.D., 2008c. Saturated hydraulic properties: Well permeameter. In: Carter, M. R., Gregorich, E.G. (Eds.), Soil Sampling and Methods of Analysis, 2nd ed. CRC Press, Boca Raton, FL, pp. 1025–1042.
Reynolds, W.D., 2016. A unified Perc Test-well permeameter methodology for absorption field investigations. Geoderma 264, 160–170. https://doi.org/10.1016/j.geoderma.2015.10.015.
Richards, L.A., 1931. Capillary conduction of liquids in porous mediums. Physics 1, 318–333.
Rudiyanto, Minasny, B., Shah, R.M., Setiawan, B.I., van Genuchten, M.T., 2020. Simple functions for describing soil water retention and the unsaturated hydraulic conductivity from saturation to complete dryness. Journal of Hydrology 588. https://doi.org/10.1016/j.jhydrol.2020.125041.
Russo, D., 1988. Determining soil hydraulic properties by parameter estimation: On the selection of a model for the hydraulic properties. Water Resources Research 24 (3), 453–459.
Schaap, M.G., Leij, F.J., 2000. Improved prediction of unsaturated hydraulic conductivity with the Mualem-van Genuchten model. Soil Science Society of America Journal 64 (3), 843–851.
Schaap, M.G., van Genuchten, M.T., 2006. A modified Mualem-van Genuchten formulation for improved description of the hydraulic conductivity near saturation. Vadose Zone Journal 5, 27–34. https://doi.org/10.2136/vzj2005.0005.
Smettem, K.R.J., Clothier, B.E., 1989. Measuring unsaturated sorptivity and hydraulic conductivity using multiple disk permeameters. Journal of Soil Science 40, 563–568.
Sternagel, A., Loritz, R., Wilcke, W., Zehe, E., 2019. Simulating preferential soil water flow and tracer transport using the Lagragian Soil Water and Solute Transport Model. Hydrology and Earth System Sciences 23, 4249–4267. https://doi.org/10.5194/hess-23-4249-2019.
Tuller, M., Or, D., 2001. Hydraulic conductivity of variably saturated porous media: Film and corner flow in angular pore space. Water Resources Research 37, 1257–1276. https://doi.org/10.1029/2000WR900328.
van Genuchten, M.Th., Leij, F.J., Yates, S.R., 1991. The RETC code for Quantifying the Hydraulic Functions of Unsaturated Soils, Version 1.0. EPA Report, U. S. Salinity Laboratory, USDA, ARS, Riverside, California.
Vandervaere, J.P., 2002. Unsaturated water transmission parameters obtained from infiltration: Three-dimensional infiltration using disk permeameters: Early-time observations. In: Dane, J.H., Topp, G.C. (Eds.): Methods of Soil Analysis, Part 1, SSSA Book Ser. 4, Madison, WI.
Vereecken, H.J., 1988. Pedotransfer functions for the generation of hydraulic properties for Belgian soils. Katholieke Universiteit Leuven, Leuven, Belgium, Ph.D. diss.
Vereecken, H., Weynants, M., Javaux, M., Pachepsky, Y., Schaap, M.G., van Genuchten, M.T., 2010. Using pedotransfer functions to estimate the van Genuchten-Mualem soil hydraulic properties: A review. Vadose Zone Journal 9 (4), 795–820.
Warrick, A.W., 1974. Time-dependent linearized infiltration. I. Point sources. Soil Science Society of America Proceedings 38, 383–386. https://doi.org/10.2136/sssaj1974.03615995003800030008x.
Warrick, A.W., 1998. In: Environmental Soil Physics. Elsevier, pp. 655–675.
Weynants, M., Vereecken, H.J., Javaux, M., 2009. Revisiting Vereecken pedotransfer functions: Introducing a closed-form hydraulic model. Vadose Zone Journal 8, 86–95. https://doi.org/10.2136/vzj2008.0062.
White, I., Sully, M.J., 1987. Macroscopic and microscopic capillary length and time scales from field infiltration. Water Resources Research 23 (8), 1514–1522.
Wooding, R.A., 1968. Steady infiltration from a shallow circular pond. Water Resources Research 4 (6), 1259–1273.
Zhang, Z.F., 2011. Soil water retention and relative permeability for conditions from oven-dry to full saturation. Vadose Zone Journal 10 (4), 1299–1308.
X. Zhang J. Zhu O. Wendroth C. Matocha D. Edwards Effect of macroporosity on pedotransfer function estimates at the field scale Vadose Zone J. 18 1 2019 1 15 180151.
Zhang, Y., Zhang, Z., Ma, Z., Chen, J., Akbar, J., Zhang, S., Che, C., Zhang, M., Cerdà, A., Lupwayi, N., 2018. A review of preferential water flow in soil science. Canadian Journal of Soil Science 98 (4), 604–618.